THE JOURNAL OF BIOLOGICAL CHEMISTRY VOL. 291, NO. 37, pp. 19573–19589, September 9, 2016
© 2016 by The American Society for Biochemistry and Molecular Biology, Inc. Published in the U.S.A.

Identification of Components of the SUMOylation Machinery in *Candida glabrata*

*ROLE OF THE DESUMOYLATION PEPTIDASE CgUlp2 IN VIRULENCE**

Received for publication, November 22, 2015, and in revised form, May 24, 2016 Published, JBC Papers in Press, July 5, 2016, DOI 10.1074/jbc.M115.706044

Rahul Gujjula[‡1,2], **Sangeetha Veeraiah**[§1], **Kundan Kumar**[‡¶], **Suman S. Thakur**[‖], **Krishnaveni Mishra**[§3], **and Rupinder Kaur**[‡4]

From the [‡]*Centre for DNA Fingerprinting and Diagnostics, Building 7, Gruhakalpa, 5-4-399/B, Nampally, Hyderabad 500001, the* [§]*Department of Biochemistry, School of Life Science, University of Hyderabad, Prof. C. R. Rao Road, Gachibowli, Hyderabad 500046, the* [¶]*Graduate Studies Program, Manipal University, Manipal, Karnataka 576104, and the* [‖]*Centre for Cellular and Molecular Biology, Habsiguda, Uppal Road, Hyderabad 500007, India*

Regulation of protein function by reversible post-translational modification, SUMOylation, is widely conserved in the eukaryotic kingdom. SUMOylation is essential for cell growth, division, and adaptation to stress in most organisms, including fungi. As these are key factors in determination of fungal virulence, in this study, we have investigated the importance of SUMOylation in the human pathogen, *Candida glabrata*. We identified the enzymes involved in small ubiquitin-like modifier conjugation and show that there is strong conservation between *Saccharomyces cerevisiae* and *C. glabrata*. We demonstrate that SUMOylation is an essential process and that adaptation to stress involves changes in global SUMOylation in *C. glabrata*. Importantly, loss of the deSUMOylating enzyme CgUlp2 leads to highly reduced small ubiquitin-like modifier protein levels, and impaired growth, sensitivity to multiple stress conditions, reduced adherence to epithelial cells, and poor colonization of specific tissues in mice. Our study thus demonstrates a key role for protein SUMOylation in the life cycle and pathobiology of *C. glabrata*.

SUMOylation, the covalent reversible conjugation of small ubiquitin-like modifier (SUMO)[5] polypeptide to lysine residues, often within the canonical consensus motif ΨK*X*E (Ψ and *X* represent a hydrophobic amino acid and any amino acid, respectively) in target proteins, is a post-translational modification that plays a key regulatory role in several cellular processes, including transcription, protein homeostasis, stress response, and development (1, 2). The process of SUMO attachment consists of the following four steps: (i) processing of the ~10-kDa precursor SUMO peptide by SUMO-specific proteases to reveal a C-terminal diglycine motif in the mature SUMO; (ii) ATP-dependent activation of the processed SUMO through the thioester bond formation between the C-terminal glycine of SUMO and the catalytic cysteine of the E1-activating enzyme; (iii) transfer of the SUMO polypeptide from the E1 enzyme to a conserved cysteine in the E2-conjugating enzyme via a thioester linkage; and (iv) E3 ligase-mediated formation of an isopeptide bond between the C-terminal glycine of the SUMO and the ϵ-amino group of the lysine residue within the conserved sequence on the target protein (2, 3). Besides the precursor SUMO maturation, the SUMO-specific peptidases are also able to hydrolyze the isopeptide bond between SUMO and SUMO-modified proteins thereby rendering the SUMOylation process reversible.

The SUMO polypeptide is ubiquitously present in all eukaryotes and highly conserved from yeast to mammals (1–3). SUMO modification of protein substrates has diverse functional consequences and range from increased protein stability to altered subcellular localization (1–3). Furthermore, deregulated expression of SUMOylation components has been implicated in several human diseases, including neurodegeneration, heart failure, cancer, diabetes, and infections by bacterial and viral pathogens (4, 5).

In the yeast *Saccharomyces cerevisiae*, SUMOylation machinery is composed of a single SUMO protein Smt3, SUMO-specific proteases Ulp1 and Ulp2, E1-conjugating heterodimeric complex Aos1-Uba2, E2-conjugating enzyme Ubc9, and four E3 ligases Siz1, Siz2, Cst9, and Mms21 (5–12). Of these proteins, Smt3, Ulp1, Aos1, Uba2, Ubc9, and Mms21 are essential for cell viability, and the substrate specificity is conferred by SUMO ligases (13, 14). Ulp2 is also known to be involved in the cleavage of poly-SUMO chains (15). SUMOylation affects about 5–10% of all yeast proteins (16–19), and SUMO-modified proteins have been implicated in ribosome function, septin ring dynamics, mRNA processing, and response to osmotic stress in *S. cerevisiae* (2, 12, 20, 21). Recently, SUMOylation has been shown to be required for thermal stress resistance in the pathogenic yeast *Candida albicans* (22).

Candida bloodstream infections, also known as candidemia, are a common occurrence in patients with immune dysfunctions and undergoing transplantation and radiation therapy

* This work was supported by the Department of Biotechnology, Government of India, Grants BT/PR7388/MED/29/650/2012 and BT/PR7123/BRB/10/1149/ 2012 (to R. K.), BT/PR11752/BRB/10/685/2009 (to K. M.), and BT/PR5145/MED/29/470/2012 (to R. K., K. M., and S. T.). The authors declare that they have no conflicts of interest with the contents of this article.

[1] Both authors contributed equally to this work.

[2] Present address: Dept. of Biochemistry, Aurora's Degree and PG College, Chikkadpally, Hyderabad 500020, India.

[3] To whom correspondence may be addressed. E-mail: krishnaveni.mishra@gmail.com.

[4] R. K. is a senior fellow of the Wellcome Trust/DBT India Alliance. To whom correspondence may be addressed. E-mail: rkaur@cdfd.org.in.

[5] The abbreviations used are: SUMO, small ubiquitin-like modifier; 5-FOA, 5-fluoroorotic acid; MMS, methyl methanesulfonate; DIC, differential interference contrast; SAP, SAF/AB, Acinus and PIAS.

TABLE 1
List of CAGLORFs identified whose orthologues in *S. cerevisiae* are involved in SUMOylation

CAGLORF	*S. cerevisiae* orthologue	% similarity	Known function in *S. cerevisiae*
SUMO activating enzymes			
CAGL0G09889g	*AOS1*	76.44	Subunit of a heterodimeric nuclear SUMO-activating enzyme, E1
CAGL0M01606g	*UBA2*	76.83	Subunit of a heterodimeric nuclear SUMO-activating enzyme, E1
SUMO-conjugating enzymes			
CAGL0M03267g	*MMS21*	59.12	SUMO ligase and component of the SMC5-SMC6 complex
CAGL0L04290g	*SIZ2*	49.62	SUMO E3 ligase
CAGL0F02783g	*SIZ1*	41.96	SUMO/Smt3 ligase
CAGL0D00814g	*UBC9*	96.18	SUMO-conjugating enzyme involved in the Smt3p conjugation pathway
SUMO protein			
CAGL0K05731g	*SMT3*	85.32	Ubiquitin-like protein of the SUMO family
DeSUMOylation peptidases			
CAGL0L08646g	*ULP1*	62.56	Protease that specifically cleaves Smt3p protein conjugates
CAGL0J02464g	*ULP2*	45.88	Peptidase that deconjugates Smt3/SUMO-1 peptides from proteins

(23, 24). Candidemia often results in prolonged hospitalization in intensive care unit, high healthcare costs, and considerable morbidity and mortality (23). During last 2 decades, the incidence rate of candidemia has increased significantly with *C. albicans* being the most prevalent species followed by *Candida glabrata* (23, 25–27). *C. glabrata* accounts for up to 29% of total *Candida* bloodstream infections with a crude mortality rate of 40–45% (26–29).

Among the known virulence factors of *C. glabrata*, glycosylphosphatidylinositol-linked adhesins, cell surface-associated proteases, robust oxidative stress response, and the ability to form biofilms and evade immune response occupy central position (30). Although SUMOylation is known to be involved in the regulation of fungal development, differentiation, and virulence (22, 31), nothing is known about its role in the pathogenesis of *C. glabrata*. Here, using the reverse genetics approach, we have identified components of the SUMOylation machinery in *C. glabrata* and show that the deSUMOylation peptidase CgUlp2 is required for biofilm formation, adhesion, and virulence of *C. glabrata*. We also report essentiality of *C. glabrata* Smt3 for cell growth and viability. Furthermore, we demonstrate for the first time a functional conservation of key SUMOylation components between *S. cerevisiae* and *C. glabrata.*

Results

Identification of Components of the SUMOylation Pathway in C. glabrata—To determine components of the SUMOylation pathway in *C. glabrata*, we performed whole proteome sequence and BLAST analyses, and identified *C. glabrata* orthologues of the proteins that are involved in SUMOylation in *S. cerevisiae* (Table 1). Orthologues of all the components could be identified, and their percent similarity across the complete sequence is shown in Fig. 1 and Table 1. SUMO and the E2 ligase Ubc9 protein are the most conserved between *C. glabrata* and *S. cerevisiae* with both showing over 85% identity (Table 1 and data not shown). Other SUMOylation components in both yeasts also showed significant sequence similarities as well as conserved architecture of various characterized domains (see Fig. 1 and data not shown). One striking difference was the absence of the SAP domain in the *C. glabrata* Siz1 ligase (see Fig. 1). The SAP domain, found in SIZ/PIAS family (Sap and Miz/protein inhibitors of activated STAT) of SUMO ligases, is implicated in DNA binding and nuclear retention (32).

In *S. cerevisiae*, deletion of the SAP domain results in reduced nuclear localization of the Siz1 ligase, whereas the full-length protein has a cell cycle-dependent localization. Although Siz1 is nuclear through most of the cell cycle stages, it relocates to the bud neck during cytokinesis, as SUMOylation of septins and other substrates at this stage is essential for completion of cell division (11, 14, 33, 34). Siz1 relocation is dependent on the C-terminal domain, whereas its nuclear retention is contingent on the SAP domain (32). Therefore, loss of this well conserved domain in CgSiz1 ligase raises the possibility of additional *C. glabrata*-specific SUMO substrates outside the nucleus.

Functional Conservation between C. glabrata and S. cerevisiae SUMO Components—Given the strong conservation of sequence and architecture of all components of the SUMOylation pathway in *C. glabrata*, we next examined whether some of the key components would functionally complement the *S. cerevisiae* mutants. For the two essential genes tested, *SMT3* and *ULP1*, we performed plasmid shuffling experiments in *S. cerevisiae* knock-outs. First, we transformed the *S. cerevisiae smt3*Δ strain carrying the Sc*SMT3* gene on a *URA3*-based vector either with a *LEU2*-based plasmid expressing the *CgSMT3* gene from the *ADH1* promoter (CKM 379) or with the *LEU2*-based vector alone. The double transformants were streaked on plates containing 5-fluoroorotic acid (5-FOA) to select for uracil auxotrophs. We found that the *S. cerevisiae smt3*Δ strain expressing *CgSMT3* survived, but the strain carrying the empty vector did not (Fig. 2*A*). This establishes that the *Scsmt3*Δ mutant could be complemented by Cg*SMT3,* and therefore it could lose the *ScSMT3*-expressing plasmid. Through similar plasmid shuffle experiments, we next showed that *CgULP1* could also complement the *Sculp1*Δ mutant (Fig. 2*B*). The *ULP2* gene is not essential for cell viability in *S. cerevisiae,* but its deletion results in growth retardation (35). As shown in Fig. 2*C*, slow growth of the *S. cerevisiae ulp2*Δ mutant was rescued by ectopic expression of the *CgULP2* gene indicative of a functional conservation between *S. cerevisiae* and *C. glabrata* Ulp2 deSUMOylase. However, CgUlp2 could not complement the telomeric silencing defect of the *Sculp2*Δ mutant as *CgULP2*-expressing *Sculp2*Δ cells did not grow on medium containing 5-fluoroorotic acid (see Fig. 2*C*). These cells carry *URA3* at the subtelomeric region of chromosome VII and would exhibit

Saccharomyces cerevisiae	*Candida glabrata*
AOS1 (347)	**CAGL0G09889g (336)**
ThiF : 16 - 345	ThiF : 12 - 335
UBA2 (636)	**CAGL0M01606g (632)**
ThiF : 2 - 437 UBA_e1_thiolCys - 246 – 363	ThiF : 4 - 442 UBA_e1_thiolCys : 248 - 368
MMS21 (267)	**CAGL0M03267g (266)**
zf-Nse : 171 - 227	zf-Nse : 174 - 230
NFI1 (726) & SIZ1 (904)	**CAGL0L04290g (754) & CAGL0F02783g (839)**
NFI1 PINIT : 152 - 289 zf-MIZ : 334 - 383 SAP : 43 - 77 **SIZ1** PINIT : 174 - 312 zf-MIZ : 357 - 406 SAP : 34 - 68	**CAGL0L04290g** PINIT : 157 - 294 zf-MIZ : 338 - 387 SAP : 18 - 52 **CAGL0F02783g** PINIT : 148 - 294 zf-MIZ : 339 - 388
UBC9 (157)	**CAGL0D00814g (157)**
UQ_con : 8 - 152	UQ_con : 8 - 151
SMT3 (101)	**CAGL0K05731g (108)**
Rad60-SLD : 22 - 92	Rad60-SLD : 30 - 100
ULP1 (621)	**CAGL0L08646g (588)**
Peptidase_C48 : 447 - 620	Peptidase_C48 : 414 - 583
ULP2 (1034)	**CAGL0J02464g (916)**
Peptidase_C48 : 456 - 675	Peptidase_C48 : 450 - 675

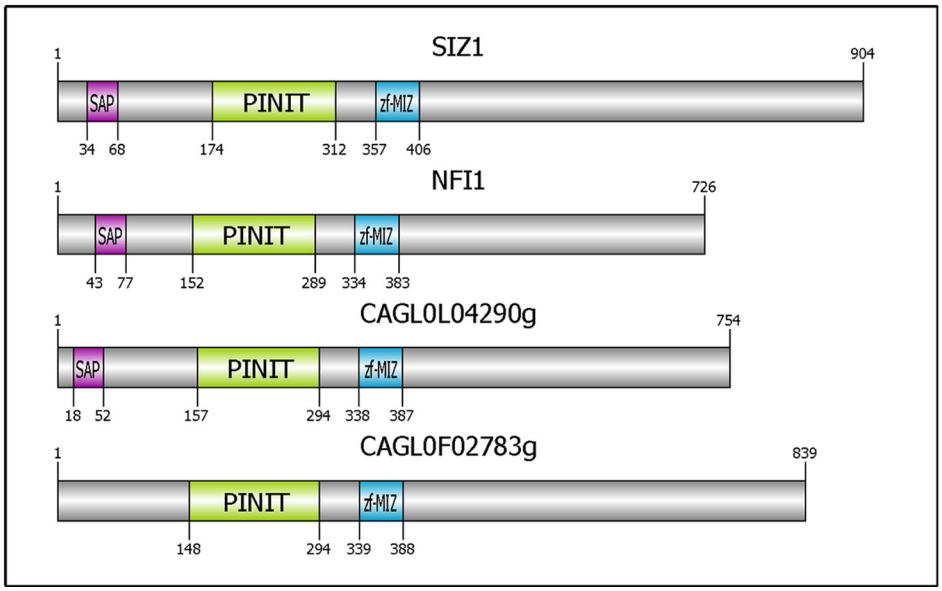

FIGURE 1. ***C. glabrata* orthologues of genes encoding components of the SUMOylation pathway.** *S. cerevisiae* proteins were retrieved from Saccharomyces Genome Database, and their orthologues in *C. glabrata* were identified using Blastp. The protein sequences were scanned for annotated domains using Pfam and HMMER. Maps of proteins along with their domains were generated using DOG.

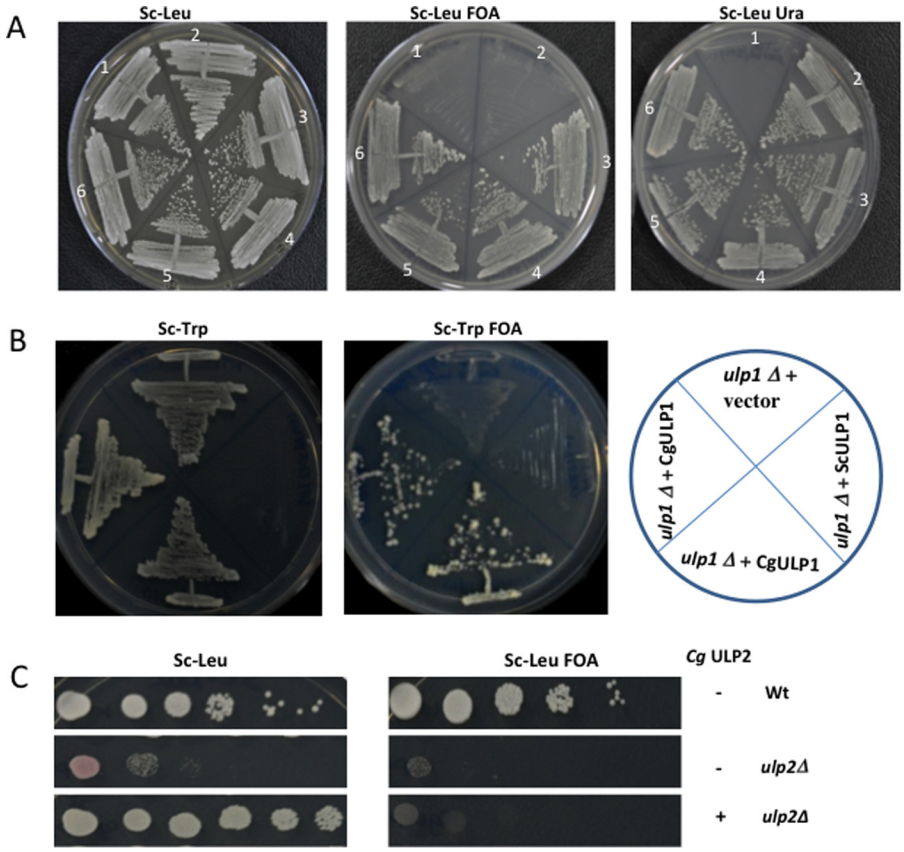

FIGURE 2. **Complementation of *S. cerevisiae* mutants with *C. glabrata* orthologues.** *A, S. cerevisiae smt3*Δ carrying *SMT3* on a plasmid with *URA3* as selectable marker was transformed with Cg*SMT3* on a Leu-marked plasmid (*3–6*) or empty Leu vector (*2*), or neither (*1*). Transformants were streaked on YPD (no selection), or Sc-Leu, Ura (selecting for both plasmids), or Sc-Leu FOA (for the absence of Ura plasmid). Only strains containing Cg*SMT3* could lose the *ScSMT3* plasmid and grow on plates containing 5-FOA. *B, S. cerevisiae ulp1*Δ carrying Sc*ULP1* on a plasmid with *URA3* as a selection marker were transformed with *CgULP1* encoded on a plasmid with *TRP1* as a selectable marker or empty Trp vector or neither. Only strains containing *CgULP1* could lose the *ScULP1* plasmid and grow on plates containing 5-FOA. *C,* Sc*ulp2*Δ with telomeric *URA3* (KRY744) was transformed with either plasmid encoding CgUlp2 or empty vector and tested for growth at 30 °C and on 5-FOA plates for silencing phenotype. *CgULP2* restores growth but not silencing in *S. cerevisiae*.

growth on FOA medium only if *URA3* expression was suppressed due to the telomere position effect. As expected, *S. cerevisiae* wild-type strain harboring the *URA3* gene at the subtelomeric locus exhibited robust growth on plates containing 5-FOA (see Fig. 2*C*). These data suggest that *CgULP2* cannot complement all functions of *ScULP2.* Of note, we could not perform complementation studies with *C. glabrata UBA2*, *AOS1*, *UBC9,* and *MMS21* genes because the corresponding heterozygous *S. cerevisiae* mutants sporulated extremely poorly (data not shown).

Subcellular Localization of C. glabrata SUMO Enzymes—In *S. cerevisiae*, SUMOylated proteins are mostly nuclear with very few proteins SUMOylated in the cytosol or other subcellular compartments. This is because most of the SUMO ligases are found in the nucleus except Siz1, which localizes to the septin ring during cell division (13, 36). To examine whether the location of SUMO enzymes was conserved between *C. glabrata* and *S. cerevisiae*, we introduced the dual His-FLAG tag sequence into *C. glabrata SMT3*, *SIZ1*, *SIZ2*, *ULP1,* and *ULP2* gene sequences, and we transformed these plasmids into either wild-type strain (for essential genes) or the respective *C. glabrata* deletion strains. Immunofluorescence analysis with anti-FLAG antibody revealed that CgSmt3 was localized uniformly across the cell suggesting that SUMO and/or SUMOylated proteins are found both in the cytosol and the nucleus (Fig. 3). The two SUMO ligases, CgSiz1 and CgSiz2, and the desumoylating enzymes, CgUlp1 and CgUlp2, were all predominantly nuclear with only CgSiz1 and CgUlp1 showing few cytosolic spots (see Fig. 3). Interestingly, the characteristic nuclear pore complex localization of ScUlp1 was not observed in CgUlp1. Thus, despite uniform distribution of SUMOylated proteins across the cell, the enzymes involved in SUMOylation and deSUMOylation are predominantly nuclear in *C. glabrata*. These findings suggest that localization of most components of the SUMOylation pathway in *C. glabrata* is similar to that in *S. cerevisiae*.

Disruption of C. glabrata ORFs That Are Potentially Involved in SUMOylation in C. glabrata—To examine the effect of perturbation of SUMOylation machinery on physiology and pathogenesis of *C. glabrata*, we sought to generate strains lacking one or more SUMO components. Of the set of nine genes shown in Table 1, we were able to create deletion strains for *CgSIZ1*, *CgSIZ2,* and *CgULP2* genes via a homologous recombination-based strategy. We also generated a double deletion strain for *CgSIZ1* and *CgSIZ2* genes to investigate the role of SUMO ligases in *C. glabrata* pathobiology. Despite several attempts, we could not delete *CgAOS1, CgUBA2, CgUBA9, CgMMS21, CgULP1,* and *CgSMT3* ORFs. Notably, *S. cerevisiae*

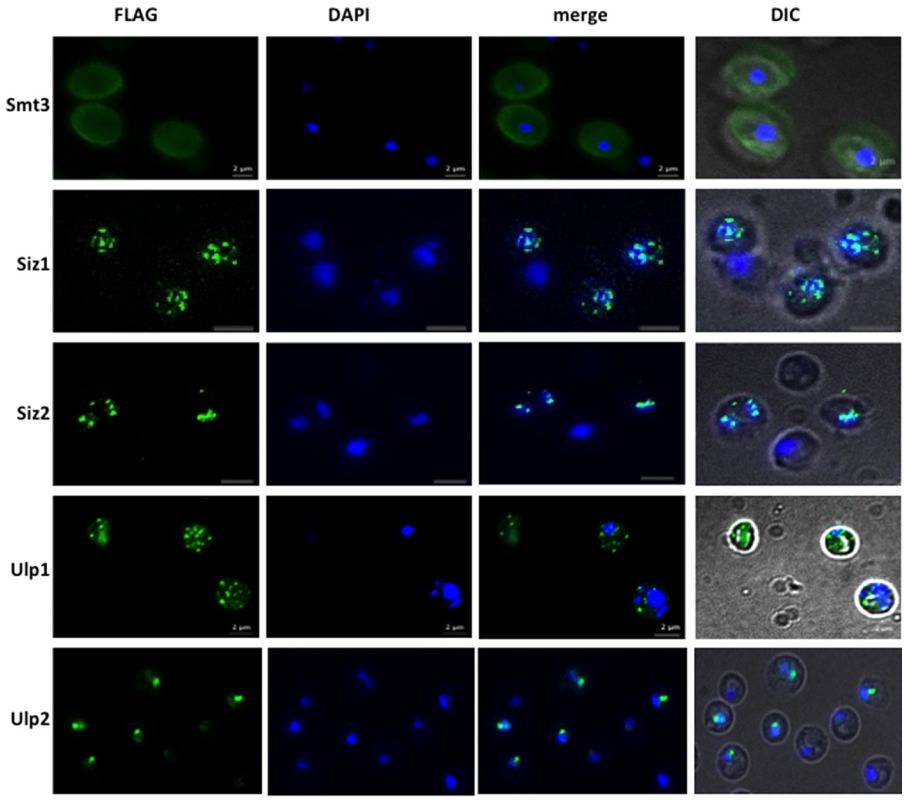

FIGURE 3. **Subcellular localization of components of SUMOylation.** Wild-type *C. glabrata* cells were transformed with plasmid encoding the indicated FLAG-tagged genes. Immunofluorescence was performed using anti-FLAG antibody (*green*), and DAPI was used to delineate the nucleus. The *4th panel* shows the merged signals in DIC to visualize the cell outline. *Bar* = 2 μm.

orthologues of these six genes are essential for cell viability (5–10). Furthermore, using the one-step disruption and plasmid loss methodologies, we could show that *CgSMT3* is required for growth *in vitro* in *C. glabrata* (data not shown).

To investigate the role of SUMOylation in cell physiology, we conducted a comprehensive phenotypic characterization of the *C. glabrata* mutants generated. Growth analysis of *Cgsiz1*Δ, *Cgsiz2*Δ, *Cgsiz1*Δ*siz2*Δ, and *Cgulp2*Δ mutants revealed that the *Cgulp2*Δ mutant grew about 18% slower than the wild-type (WT) strain in rich medium (Fig. 4*A*). The *Cgulp2*Δ mutant exhibited highly attenuated growth at 42 °C and in medium containing caffeine and non-fermentable carbon sources (glycerol, oleic acid, and ethanol) (Fig. 4, *B* and *C*). Compared with WT cells, the *Cgulp2*Δ mutant was more susceptible to the DNA-alkylating agent methyl methanesulfonate (MMS), replication fork staller hydroxyurea, thymine dimer-inducing ultraviolet (UV) radiation, and oxidative stress-inducing agent hydrogen peroxide (see Fig. 4*B*). Elevated sensitivity of the *Cgulp2*Δ mutant to aforementioned stresses was complemented by ectopic expression of the *CgULP2* gene, indicating that these effects were specifically induced by the absence of *CgULP2* (see Fig. 4*B*). Contrary to the *Cgulp2*Δ mutant, growth of the *Cgsiz1*Δ mutant remained unaffected under diverse stressful conditions, *viz.* DNA damage (MMS, camptothecin, and hydroxyurea), oxidative (hydrogen peroxide and menadione), thermal (37 and 42 °C), varied pH values (low (2.0) and neutral (7.0) pH), cell wall (caffeine), cell membrane SDS, non-fermentable carbon sources, and antifungal drug (fluconazole and caspofungin) stresses (see Fig. 4, *B* and *C* and data not shown). Interestingly, the *Cgsiz2*Δ and *Cgsiz1*Δ*siz2*Δ mutants displayed sensitivity to both UV and MMS, which could be rescued by ectopic expression of the *CgSIZ2* gene (see Fig. 4*B*). Expression of *CgSIZ1* partially restored slow growth of the *Cgsiz1*Δ*siz2*Δ mutant in MMS-supplemented medium and upon UV treatment (see Fig. 4*B*). Altogether, these data implicate CgSiz2 and CgUlp2 in survival of DNA damage and thermal, oxidative, and DNA damage stresses, respectively.

Disruption of CgULP2 Rendered C. glabrata Cells Hypoadherent to Lec2 Ovary Epithelial Cells—During our phenotype profiling analysis, we noticed that about 5% of the *Cgulp2*Δ mutant population displayed elongated pseudohypha-like structures after 48 h of growth in the YPD medium (Fig. 5*A*). To investigate whether this change in morphology is due to altered cell wall composition, we examined sensitivity of the *Cgulp2*Δ mutant to digestion with zymolyase, which hydrolyzes β-glucan in the cell wall. The fungal cell wall is a complex and dynamic structure and consists of an inner layer of β-glucan-chitin complex and an outer layer of heavily *O*- and *N*-glycosylated mannoproteins (37). Compared with WT cells, the *Cgulp2*Δ mutant displayed resistance to zymolyase digestion, which was reversed upon ectopic expression of the *CgULP2* gene in the mutant (Fig. 5*B*). Furthermore, cell wall chitin analysis revealed 1.5-fold elevated chitin content in the *Cgulp2*Δ mutant compared with WT cells (Fig. 5*C*). Consistently, staining with calcofluor white, which binds to chitin in the cell wall, showed a diffused signal along the cell wall in the *Cgulp2*Δ mutant compared with bud scar-limited staining of WT cells

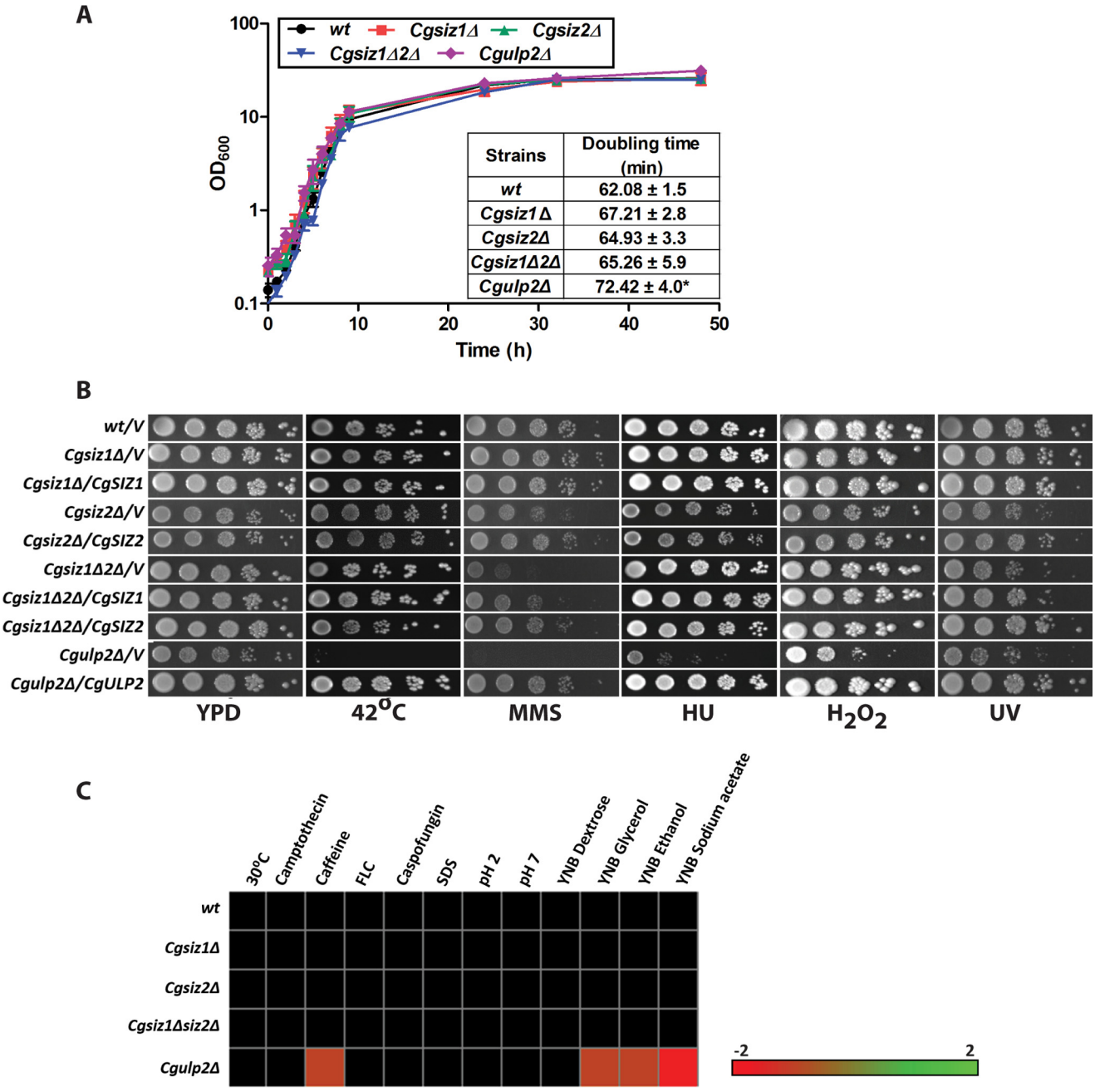

FIGURE 4. **CgUlp2 is required for survival of thermal and DNA damage stress.** *A,* growth curve analysis. Overnight-grown cultures of indicated *C. glabrata* strains were inoculated into the YPD medium to an initial A_{600} of 0.1. Absorbance at 600 nm was recorded over a 48-h time course at indicated time intervals. Data represent mean ± S.E. of three to five independent experiments. Doubling times were calculated during the exponential phase of growth and are presented on the *bottom right side* of the graph. Statistical analysis was performed using an unpaired, two-tailed, Student's *t* test (*, $p \leq 0.05$). *B,* serial dilution-spotting assay to assess the growth under indicated stress conditions. 3 μl of 10-fold serial dilutions of overnight-grown and 1.0 A_{600}-normalized cultures of indicated *C. glabrata* strains were spotted on different media. Plate images were captured after 2 days of incubation at 30 °C. Methylmethanesulfonate (*MMS*), hydroxyurea (*HU*) and hydrogen peroxide (H_2O_2) were used at the concentrations of 0.03%, 50 mM, and 50 mM, respectively. To check sensitivity to ultraviolet radiation, 3 μl of 10-fold serial culture dilutions was spotted on the YPD medium, and the plate was exposed to 40 J/m^2 UV radiation at 256 nm before incubation at 30 °C. *C,* heat map illustrating cell growth in the presence of diverse stress-causing agents. 3 μl of 10-fold serial dilutions of overnight YPD medium-grown and 1.0 A_{600}-normalized cultures of indicated *C. glabrata* strains were spotted on different media. Growth profiles, recorded after 1–8 days of incubation, are color-coded and indicated at the *bottom*. *Columns* correspond to various growth condition mutants and *rows* to mutants. Stressful conditions used were as follows: DNA damage stress (camptothecin; 10 mM); cell wall stress (caffeine; 10 mM); antifungal stress (fluconazole (FLC; 16 μg/ml) and caspofungin (75 ng/ml)); membrane stress (SDS; 0.005%); varied pH stress (pH 2.0 and 7.0); and utilization of alternative carbon sources (glycerol (3%), ethanol (2%), and sodium acetate (2%)).

(Fig. 5*D*). Overall, these findings are indicative of an altered cell wall architecture in the *Cgulp2*Δ mutant.

Cell wall integrity in *C. glabrata* is maintained by protein kinase C (PKC)-mediated signal transduction pathway, and mutants with cell wall defects have previously been reported to exhibit constitutively activated PKC signaling cascade (38). To examine the status of the PKC-dependent signaling pathway in the *Cgulp2*Δ mutant, we checked phosphorylation levels of CgSlt2, which is the terminal mitogen-activated protein kinase (MAPK) of the PKC pathway, in the mutant. As shown in Fig.

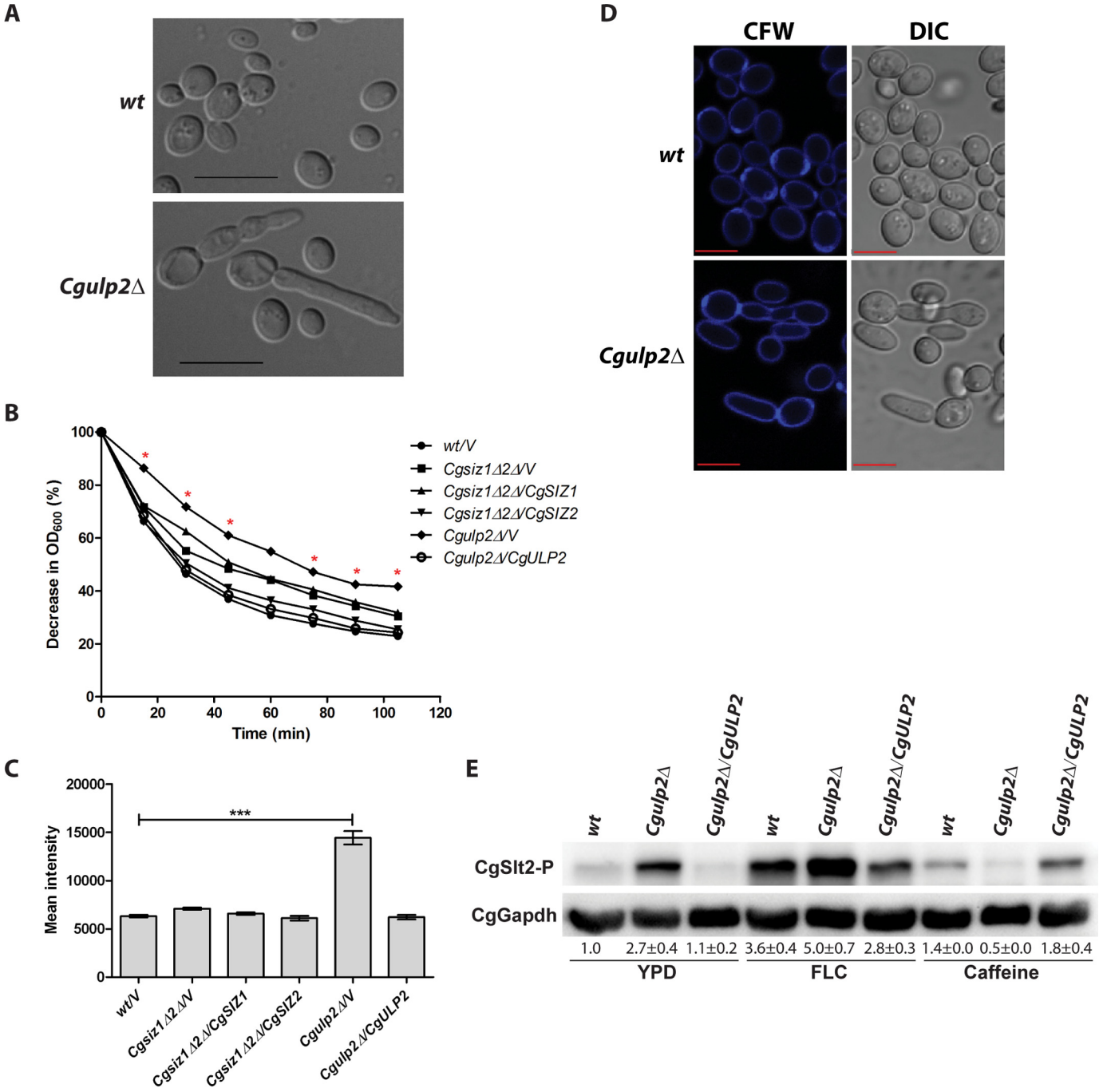

FIGURE 5. **Cell wall architecture is altered in the *Cgulp2*Δ mutant.** *A, Cgulp2*Δ mutant displayed pseudohyphal structures. Representative DIC of WT and *Cgulp2*Δ mutant grown in the YPD medium for 72 h. *B,* zymolyase digestion assay. Log phase cultures of indicated *C. glabrata* strains were treated with 50 μg/ml zymolyase, and absorbance at 600 nm was recorded at regular time intervals. Initial A_{600} of the cultures was considered as 100%, and data (means of three (*Cgsiz1*Δ*2*Δ*/CgSIZ2* and *Cgulp2*Δ*/V* strains), four (*Cgsiz1*Δ*2*Δ*/V* and *Cgsiz1*Δ*2*Δ*/CgSIZ1* strains), and five (WT*/V* and *Cgulp2*Δ*/CgULP2* strains) independent experiments) are plotted as percentage of the starting A_{600}. Statistical analysis was performed using an unpaired, two-tailed, Student's *t* test (*, $p \leq 0.05$). Statistically significant differences between WT and the *Cgulp2*Δ mutant are marked. *C,* cell wall chitin measurement. Log phase cultures of indicated *C. glabrata* strains were stained with 25 μg/ml calcofluor white (*CFW*), and fluorescence intensity was measured by flow cytometry. Signal intensity mean values ± S.E. represent data from three independent experiments. Unpaired, two-tailed, Student's *t* test is shown (***, $p \leq 0.001$). Statistically significant differences between WT and the *Cgulp2*Δ mutant are marked. *D,* representative confocal images illustrating calcofluor white (*CFW*)-stained cell walls of log phase cultures of WT and *Cgulp2*Δ mutant. *Scale bar,* 10 μm; DIC, differential interference contrast. *E,* Western blotting of CgSlt2 phosphorylation in indicated *C. glabrata* strains grown in YPD medium, YPD medium containing 16 μg/ml fluconazole (*FLC*), and 10 mM caffeine for 4 h at 30 °C. Whole cell protein extracts were prepared by glass bead lysis and quantified using the Thermo Scientific Pierce BCA protein assay kit. 30 μg of protein was separated on SDS-PAGE, and Western blots were developed with an anti-phospho-ERK1/2 MAPK (Thr^{202}/Tyr^{204}) antibody. Individual band intensity was quantified using the ImageJ software. CgSlt2 phosphorylation signal was normalized to the corresponding CgGapdh signal in each lane, and results, representative of at least three independent experiments, are presented as fold change (± S.E.) in phosphorylation levels compared with CgSlt2 phosphorylation in YPD-grown wild-type cells (considered as 1).

5*E*, the *Cgulp2*Δ mutant exhibited high levels of phosphorylated CgSlt2 compared with wild type and complemented strains indicating a constitutively active PKC-mediated cell wall integrity pathway. Furthermore, consistent with earlier studies, *C. glabrata* WT cells responded to the antifungal fluconazole and the cell wall stressor caffeine by activating the PKC cascade (see Fig. 5*E*). However, caffeine treatment, instead of activating the PKC pathway, resulted in down-regulation of CgSlt2 phosphorylation in the *Cgulp2*Δ mutant (see Fig. 5*E*). Of note, the *Cgulp2*Δ mutant was fully proficient in activation of the PKC pathway upon fluconazole exposure (see Fig. 5*E*). These data indicate that lack of *CgULP2* adversely affects the ability of *C. glabrata* cells to respond to the cell wall stressor caffeine. Importantly, these findings are in accordance with regular and elevated sensitivity of the *Cgulp2*Δ mutant to fluconazole and caffeine, respectively (see Fig. 4*C*).

Next, to investigate the effect of altered cell wall structure on the adhesion capacity of the *Cgulp2*Δ mutant, we examined the ability of *Cgulp2*Δ to adhere to Lec2 ovary epithelial cells. As a control, adherence assays were also carried out with *Cgsiz1*Δ, *Cgsiz2*Δ, and *Cgsiz1*Δ*siz2*Δ mutants, all of which displayed no detectable cell wall abnormalities (see Fig. 5, *B* and *C*). As shown in Fig. 6*A*, the *Cgulp2*Δ mutant displayed 2-fold less adherence to epithelial cells compared with that of the WT cells, which was again restored back to WT levels in the *Cgulp2*Δ-complemented strain. The hypo-adherence of the *Cgulp2*Δ mutant was unexpected and found to be, in part, due to a 3–4-fold reduced expression of two epithelial adhesin-encoding genes *EPA1* and *EPA6* in the mutant (Fig. 6*B*). Notably, Epa1 and Epa6 belong to a family of at least 23 cell wall adhesins that mediate adherence of *C. glabrata* cells to host epithelial cells (39–41). Epa6 has also been shown to be pivotal to biofilm formation *in vitro* (42). To examine the effect of *EPA6* transcript levels on biofilm formation, we measured the ability of WT, *Cgulp2*Δ, and *Cgulp2*Δ-complemented strains to make biofilm on polystyrene-coated plates. We observed that the *CgULP2* disruption led to a 50% reduction in the biofilm formation capacity of *C. glabrata* cells (Fig. 6*C*). Collectively, these data indicate that CgUlp2 plays a role in regulated expression of adhesin-encoding genes, biofilm formation, and maintenance of cell wall architecture.

Perturbation of SUMOylation Affects Growth of C. glabrata—SUMOylation of protein targets is regulated in part by recruitment of SUMO ligases and isopeptidases to specific subcellular sites at specific instances (13, 43). Therefore, we tested the effect of an additional 1–2 copies of E3 SUMO ligases and isopeptidases on the physiology of *C. glabrata* by transforming WT cells with the pRK74 plasmid expressing *CgSIZ1*, *CgSIZ2*, *CgMMS21*, *CgULP1*, or *CgULP2* genes from the *PGK1* promoter. We found that although additional copies of Cg*SIZ1*, Cg*MMS21*, Cg*ULP1*, or Cg*ULP2* genes had no measurable effect on growth (data not shown), an additional copy of the Cg*SIZ2* gene resulted in perturbed growth (Fig. 7). This effect was specific to the minimal medium as *C. glabrata* WT cells carrying *CgSIZ2*-expressing plasmid exhibited normal growth on the YPD medium (see Fig. 7). Intriguingly, additional copy of Cg*SIZ2* also rendered cells sensitive to MMS, again in the minimal medium (see Fig. 7). Because the CgUlp2 deletion also caused similar phenotypes, albeit in all media, including YPD

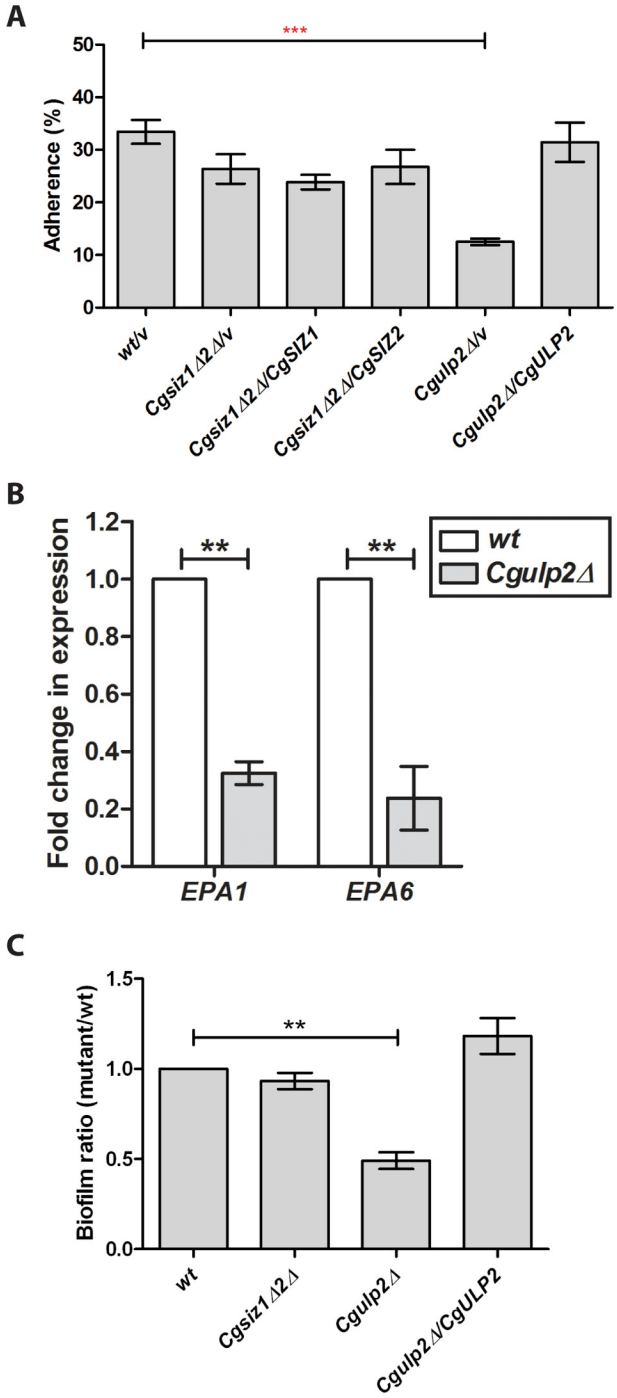

FIGURE 6. ***Cgulp2*Δ mutant displayed reduced adherence to the Lec2 epithelial cells.** *A*, adherence of CAA medium-grown, ^{35}S-labeled (Met/Cys, 65:25) *C. glabrata* strains to formaldehyde-fixed Lec-2 ovary epithelial cells. Data represent means ± S.E. of three to five independent experiments. Unpaired, two-tailed, Student's *t* test (***, $p \leq 0.001$). *B*, quantitative PCR analysis of *EPA1* and *EPA6* gene expression in wild-type and *Cgulp2*Δ mutant. Data (mean of three independent experiments ± S.E.) were normalized to an internal *CgGAPDH* mRNA control and represent fold change in expression upon *CgULP2* disruption. Paired two-tailed, Student's *t* test (**, $p \leq 0.01$) is shown. *C*, biofilm formation of indicated *C. glabrata* strains. Cells were grown in RPMI 1640 medium containing 10% FBS for 48 h in a polystyrene 24-well plate. Cells were stained with crystal violet (0.4% in 20% (v/v) ethanol solution) for 45 min followed by complete destaining with 95% ethanol. Absorbance at 595 nm was recorded to measure the amount of the crystal violet stain in ethanol. Data represent means ± S.E. of three independent experiments. **, $p \leq 0.01$; two-tailed paired Student's *t* test.

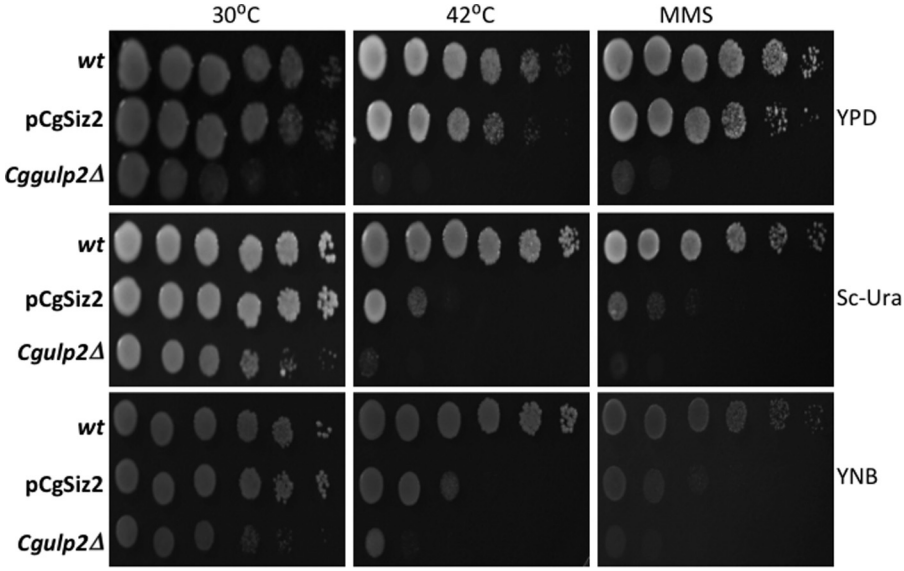

FIGURE 7. **Elevated dosage of Siz2 affects growth.** Wild-type *C. glabrata* strains were transformed with a *URA3* marked plasmid encoding CgSiz2 or empty vector and were tested for growth by spotting 5 ml of 10-fold serially diluted cultures at 30 and 42 °C or on plates containing 0.03% MMS. Elevated dosage of *CgSIZ2* impairs growth at 42 °C and MMS on minimal media. *Cgulp2*Δ, which is sensitive to temperature and MMS, is shown for comparison.

(see Figs. 4*B* and 7), we speculate that this may either be due to the increased SUMOylation of a critical substrate by CgSiz2 or absence of deSUMOylation of that substrate in the *Cgulp2*Δ mutant.

Global SUMOylation Pattern Is Altered in C. glabrata Mutants Lacking SUMO Ligases and deSUMOylase—To detect the SUMO proteome of *C. glabrata*, we tagged the CgSmt3 protein with His_6 and FLAG epitopes at the N terminus (hereafter referred to as "dual tagged Smt3") and performed Western blots on whole cell extracts of the *Cgsmt3*Δ mutant complemented either with CgSmt3 or dual tagged CgSmt3 using anti-FLAG antibody. The dual tagged CgSmt3 was able to complement the viability defect of the *Cgsmt3*Δ mutant. As seen in Fig. 8*A*, we could detect multiple proteins only in the presence of FLAG-labeled CgSmt3 confirming that the tagged CgSmt3 was conjugated to cellular proteins. Although global protein SUMOylation was reduced in *Cgsiz1*Δ and *Cgsiz2*Δ mutants, the *Cgsiz1*Δ*siz2*Δ double mutant had hardly any detectable SUMOylated proteins (see Fig. 8*A*). Furthermore, the presence of differentially SUMOylated proteins in *Cgsiz1*Δ and *Cgsiz2*Δ mutants is indicative of substrate specificity of CgSiz1 and CgSiz2 ligases (see Fig. 8*A*). Unexpectedly, in the *Cgulp2*Δ mutant, we could detect neither SUMOylated proteins nor free SUMO. Next, we examined the SUMOylation pattern in *C. glabrata* WT cells expressing additional copies of CgSiz1, CgSiz2, CgUlp1, and CgUlp2 enzymes. CgSiz1 or CgSiz2 hyperexpression led to increased protein SUMOylation, with CgSiz2 being more effective than CgSiz1 with several high molecular weight SUMOylated proteins (Fig. 8*B*). Interestingly, elevating the dosage of the SUMO peptidases, CgUlp1 and CgUlp2, did not reduce the SUMOylated proteins (see Fig. 8*B*) suggesting that deSUMOylation is very well regulated.

The result that the *Cgulp2*Δ mutant contains neither any SUMOylated proteins nor free SUMO is intriguing. We expected to see accumulation of SUMO-conjugated proteins in the absence of a deSUMOylase. There are two possible explanations for this observation as follows: first, as in *Aspergillus nidulans* (31), CgUlp2 is the SUMO-processing enzyme, and therefore, in its absence, no SUMOylation can be detected. Alternatively, increased accumulation of polySUMOylated proteins in the *Cgulp2*Δ mutant leads to their degradation by the SUMO-dependent ubiquitination pathway. To test whether CgUlp2 is required for SUMO-processing, we made a *CgSMT3* construct that encodes *SMT3* without the last four amino acids and terminating with the diglycine motif that could be directly used for conjugation to substrates. This construct was expressed in *Cgulp2*Δ mutant cells. We found that expressing mature SUMO improved the growth

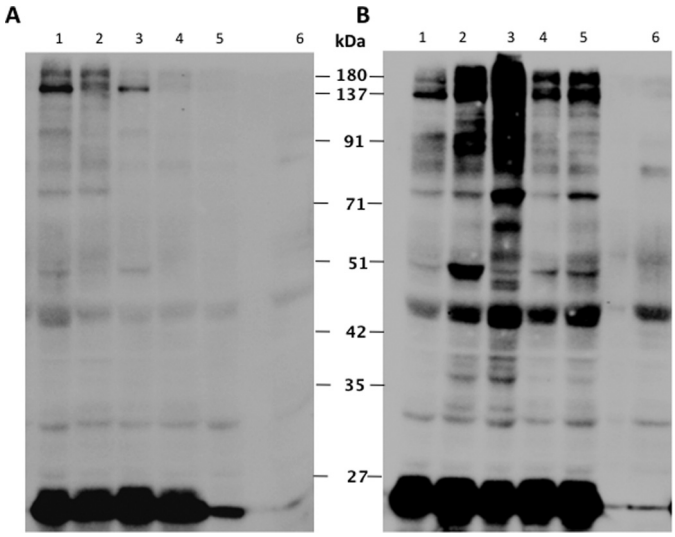

FIGURE 8. **Changes in global SUMOylation pattern upon altered dosage of SUMOylation components.** Whole cell protein extracts were separated by SDS-PAGE, and Western blotting analysis was developed with anti-FLAG antibody. *A, lane 1*, WT; *lane 2, Cgsiz1*Δ; *lane 3, Cgsiz2*Δ; *lane 4, Cgsiz1*Δ*siz2*Δ; *lane 5, Cgulp2*Δ; and *lane 6*, WT (no tag). *B, lane 1*, WT; *lane 2*, WT + pCgSiz1; *lane 3*, WT + pCgSiz2; *lane 4*, WT + pCgUlp1; *lane 5*, WT + pCgUlp2; and *lane 6*, WT (no tag).

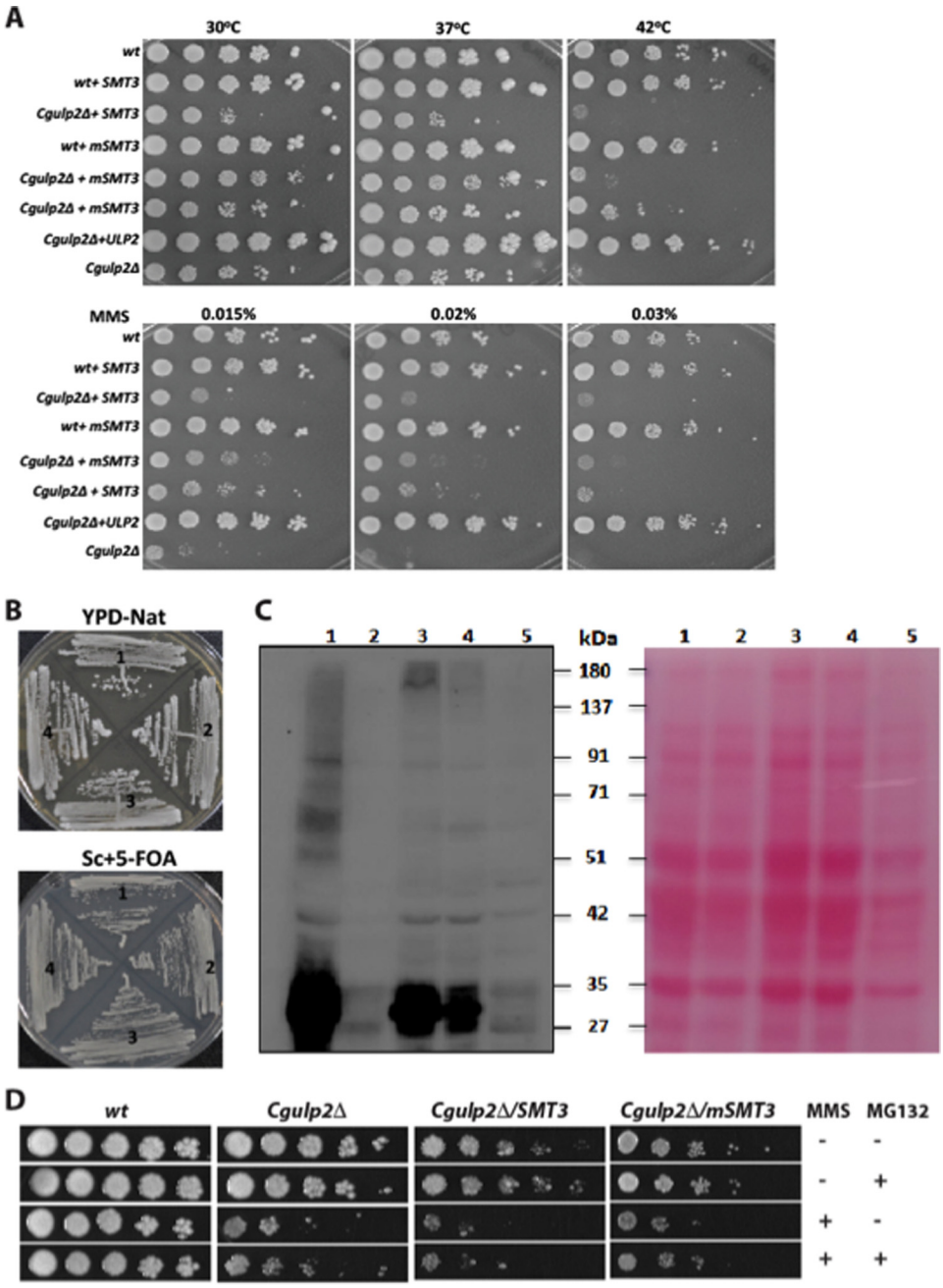

FIGURE 9. **Severity of the *Cgulp2*Δ mutant phenotype is partly reduced by mature SUMO.** *A,* copy of either empty vector or full-length *CgSMT3* (*SMT3*) or *CgSMT3* encoding mature SUMO (*mSMT3*) was introduced in the *Cgulp2*Δ mutant and WT cells. Cells were tested for growth at non-permissive temperatures and plates containing MMS as indicated by spotting 5 μl of 10-fold serially diluted cultures. Improved survival of the *Cgulp2*Δ mutant could be observed in both conditions. *B, Cgsmt3*Δ (YRK1022) was transformed with either dual-tagged *SMT3* (*1* and *2*; pCKM405) or dual-tagged *m-SMT3* (*3* and *4*; pCKM469) and tested for complementation of *SMT3* function by loss of WT-*CgSMT3*. YPD-Nat growth indicates presence of the pCN-PDC1 plasmid, and growth on 5-FOA plates indicates ability to lose the WT-*CgSMT3* carried on pGRB2.2 plasmid in the *Cgsmt3*Δ strain. *C,* total protein extracts were made from indicated *C. glabrata* strains, and the SUMOylation pattern was analyzed as described above. The mature SUMO but not the full-length SUMO could be detected clearly in the *Cgulp2*Δ mutant. Ponceau S-stained membrane is displayed as a loading control. *D,* indicated *C. glabrata* strains were grown overnight in the YNB medium containing 0.1% proline as a sole nitrogen source at 30 °C and 200 rpm. Cells were harvested; A_{600} was adjusted to 0.5 with fresh media containing 0.003% SDS and incubated for 4 h. Cultures were transferred into a 96-well plate containing 100 μl of YNB-proline media and 300 μM MG132 and incubated at 30 °C at 175 rpm. After a 2 h incubation, MMS (0.045%) was added to the media and grown for 3 h. Cultures were 10-fold serially diluted, and a 3 μl volume was spotted on YPD medium. Plate images were captured after 48 h of incubation at 30 °C.

of *Cgulp2*Δ measurably but not up to wild-type levels (Fig. 9*A*). Similarly, it also conferred improved resistance to MMS; in both cases, merely adding additional copies of full-length *CgSMT3* did not improve growth (see Fig. 9*A*). We confirmed that the mature SUMO complemented the *Cgsmt3*Δ phenotype using the plasmid shuffle assay described earlier (Fig. 9*B*). Western blot analyses revealed that now we could detect free SUMO and a very slight increase in the SUMO proteome (Fig. 9*C*). These observations together suggest that either providing mature SUMO improves the stability of critical SUMOylated proteins or having mature free SUMO improves survival by non-covalent associations.

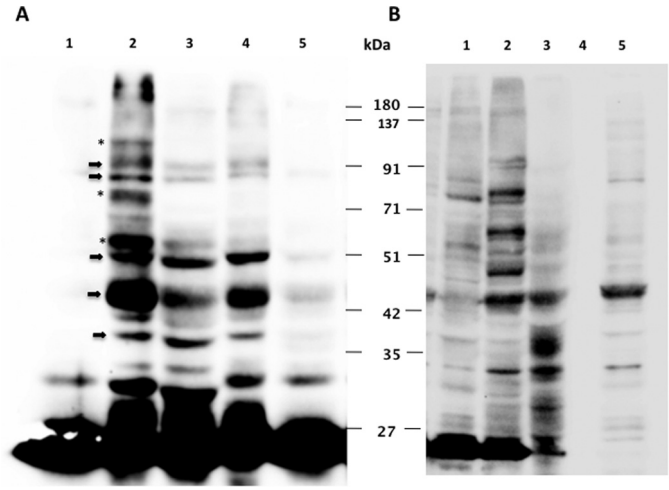

FIGURE 10. **Stress induces changes in SUMOylation.** *A,* log phase cultures of *C. glabrata* were treated for 4 h with 10% ethanol (*lane 2*) or 0.075% MMS (*lane 3*) or 150 mM hydroxyurea (*lane 4*) or 64 μg/ml fluconazole (*lane 5*), and total protein extracts were made, and Western blot analysis was developed with anti-FLAG antibody. *Lane 1* is untreated. *Asterisks* indicate those proteins that are SUMOylated under all stress conditions, and *arrows* indicate those that are unique to alcohol treatment. *B,* THP1 macrophages were infected with *C. glabrata* strains, and internalized *C. glabrata* strains were extracted, and total protein extracts were made. *Lane 1* is *smt3*Δ complemented with tagged *SMT3* grown in RPMI 1640 medium; *lane 2* is *C. glabrata* extracted from macrophages, and *lane 3* is uninfected macrophages. *Lane 5* depicts YPD grown *C. glabrata* extract for comparison.

To address the other possibility that increased accumulation of polySUMOylated proteins in the *Cgulp2*Δ mutant leads to their degradation by the ubiquitin-proteasome pathway, we checked the SUMOylation pattern in *Cgulp2*Δ cells treated with the proteasome inhibitor MG132, but we did not find any increase in SUMOylation levels of proteins (data not shown). Consistently, MG132 treatment could only marginally rescue the MMS sensitivity of the *Cgulp2*Δ mutant (Fig. 9*D*). Of note, no further rescue of MMS sensitivity was observed upon expression of full-length or mature SUMO protein in the *Cgulp2*Δ mutant (see Fig. 9*D*). These data suggest that the hyperactivated ubiquitin-proteasome proteolytic pathway is unlikely to be the sole cause of overall reduction in SUMOylation levels in the *Cgulp2*Δ mutant.

Ethanol Stress and Macrophage Internalization Induce Accumulation of SUMO-conjugated Proteins in C. glabrata—SUMOylation has previously been implicated in the cellular response to diverse stresses (42, 43). We therefore checked alterations in the SUMO proteome of *C. glabrata* cells upon a 4-h exposure to DNA damage (0.075% MMS), ethanol (10%), oxidative (150 mM H_2O_2) stresses, and antifungal (fluconazole 64–100 μg/ml) stress. Western blot analysis using anti-FLAG antibody revealed that treatment with alcohol led to increased SUMOylation of several proteins, whereas MMS and H_2O_2 exposure showed increased SUMOylation for a few proteins (Fig. 10*A*) suggesting that SUMO conjugation of multiple proteins is a part of cellular stress response in *C. glabrata*. Notably, contrary to expectations, *C. glabrata* SUMOylation-defective mutants, *Cgsiz1*Δ, *Cgsiz2*Δ, *Cgsiz1*Δ*siz2*Δ, and *Cgulp2*Δ mutants, did not exhibit elevated susceptibility to ethanol stress (data not shown), which could be reflective of functional redundancy among components of the SUMOylation machinery in *C. glabrata*.

C. glabrata cells encounter several stressful conditions in the internal milieu of macrophages, including the nutrient-limiting reactive oxygen species-generating environment (30). To gain insights into whether intracellular survival/proliferation of *C. glabrata* cells in macrophages involves SUMO proteome modifications, we performed co-incubation assays. Macrophages derived from the human monocytic cell line THP-1 were co-incubated for 8 h with dual tagged *SMT3*-expressing *C. glabrata* cells, and the internalized *C. glabrata* were harvested. Total protein from these yeast cells was compared with RPMI 1640 medium-grown *C. glabrata* cells for any changes in SUMO proteome. As seen in Fig. 10*B*, in comparison with RPMI 1640 medium-grown *C. glabrata* cells, macrophage-internalized *C. glabrata* cells showed several prominently SUMOylated proteins. This establishes that to survive and multiply within macrophages, several *C. glabrata* proteins are SUMOylated.

CgUlp2 Is Required for Virulence in the Murine Model of Systemic Candidiasis—Next, to examine the interaction of *C. glabrata* strains with altered levels of SUMOylated proteins with host immune cells, we infected human THP-1 macrophages with wild type, *Cgsiz1*Δ, *Cgsiz2*Δ, *Cgsiz1*Δ*siz2*Δ, and *Cgulp2*Δ mutants, and we studied their intracellular growth behavior via colony-forming unit (CFU) assay. Of note, *C. glabrata* wild-type cells are known to multiply in macrophages (30). All strains were phagocytosed by macrophages at the same rate of ~70–85% (wild type (73%), *Cgsiz1*Δ (84%), *Cgsiz2*Δ (74%), *Cgsiz1*Δ*siz2*Δ (80%), and *Cgulp2*Δ (71%)). However, compared with 4–6-fold intracellular replication of WT and *Cgsiz* mutants, the *Cgulp2*Δ mutant exhibited no increase in CFUs after 24 h of co-incubation with THP-1 macrophages (Fig. 11*A*). A 24-h time course analysis in the RPMI 1640 medium revealed 6-fold lower CFUs for the *Cgulp2*Δ mutant (Fig. 11*B*) suggesting that the impaired intracellular proliferation of the mutant could be due to both the diminished capacity to grow under tissue culture conditions and the elevated susceptibility to oxidative stress. Notably, *C. glabrata* strains expressing additional copies of *CgSIZ1, CgSIZ2*, *CgULP1,* and *CgULP2* genes were able to undergo 5–6-fold multiplication in THP-1 macrophages (WT/*CgSIZ1* (6.1-fold), WT/*CgSIZ2* (4.5-fold), WT/*CgULP1* (5.7-fold), and WT/*CgULP2* (5.6-fold)), indicating that increased dosage of SUMO ligases and deSUMOylases had no effect on intracellular proliferation.

Next, to investigate whether components of the SUMOylation machinery are required for virulence of *C. glabrata*, we examined fungal burden in BALB/c mice infected intravenously either with the wild-type or the *Cgsiz1*Δ*siz2*Δ and *Cgulp2*Δ mutant strains. Approximately, 10- and 8-fold lower yeast CFUs were recovered from the kidneys and liver, respectively, of the mice infected with the *Cgulp2*Δ mutant compared with CFUs retrieved from corresponding organs of the WT-infected mice (Fig. 11, *C* and *D*). Ectopic expression of the *CgULP2* gene restored the organ fungal burden in the *Cgulp2*Δ-infected mice (see Fig. 11, *C* and *D*). Of note, no statistically significant differences in the fungal burden were seen between the spleen of WT- and *Cgulp2*Δ-infected mice (Fig. 11*E*).

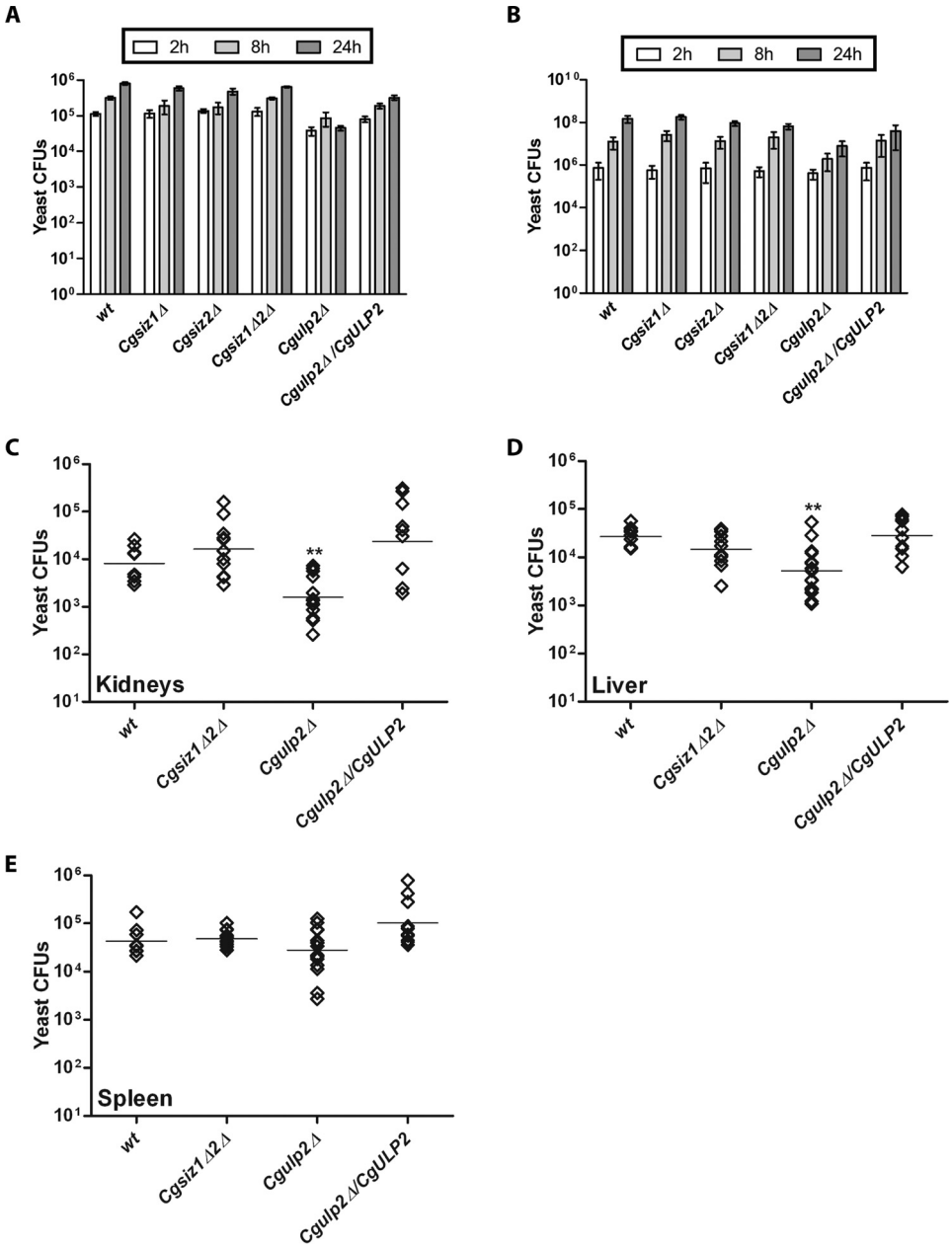

FIGURE 11. **CgUlp2 desumoylase is required for virulence in the murine model of disseminated candidiasis.** *A,* 1×10^5 cells of indicated *C. glabrata* strains were added to phorbol 12-myristate 13-acetate-differentiated THP1 cells (1×10^6) in a 24-well plate followed by removal of non-phagocytosed *C. glabrata* cells after 2 h. At indicated time intervals, intracellular yeast cells were recovered by lysing THP-1 cells in water and plating appropriate dilutions of lysates on the YPD medium. Yeast colonies were counted after 24–48 h of incubation at 30 °C. Data represent the mean of three to four independent analyses (± S.E.). *B,* cell proliferation of the indicated *C. glabrata* strains in the RPMI 1640 medium containing 10% FBS (fetal bovine serum) medium was assessed by CFU assay. Data represent the means of three to four independent analyses (±S.E.). *C–E,* 6–8-week-old female BALB/c mice were infected intravenously with 4×10^7 cells of indicated *C. glabrata* strains and sacrificed 7 days post-infection. *Diamonds* represent the CFUs recovered from target organs kidney (*C*), liver (*D*), and spleen (*E*) for individual mice. *Horizontal line* represents the geometric mean ($n = 8$–14) of CFUs per organ for all mice in one group. Statistically significant differences in CFUs between WT and mutant strains are indicated (**, $p \leq 0.01$; Mann–Whitney test).

Importantly, statistically similar yeast CFUs were obtained from all three target organs of WT- and *Cgsiz1*Δ*siz2*Δ-infected mice (see Fig. 11, *C–E*). Together, these data indicate an organ-specific role for the CgUlp2 deSUMOylase and dispensability of CgSiz1 and CgSiz2 SUMO ligases in survival of *C. glabrata* in the murine model of disseminated candidiasis.

Discussion

In this work, we have initiated studies to understand the importance of protein SUMOylation in the pathobiology of *C. glabrata*. First, we identified components of the SUMOylation machinery in *C. glabrata* based on homology with *S. cerevisiae*. Second, we performed complementation studies in *S. cerevisiae* to confirm the predicted activities. Third, we generated *C. glabrata* deletion strains for non-essential SUMOylation genes and examined the effects of perturbed SUMOylation on stress response and survival *in vivo*. Finally, we demonstrated the essentiality of CgSmt3 for cell growth in *C. glabrata*. Our studies firmly establish that SUMOylation, like in *S. cerevisiae*, is essential in *C. glabrata*. This is different

from other yeast/fungi like *Schizosaccharomyces pombe, A. nidulans,* and *C. albicans*, where *SMT3* is not essential for survival (22, 31, 44). We also speculate that the essential SUMO conjugation in *C. glabrata* may be carried out by the CgMms21 because the *Cgsiz1siz2*Δ mutant is viable (see Fig. 4*A*) and the *Cgmms21*Δ mutant could not be generated. In addition, we could not create knock-outs for genes encoding SUMO-processing enzyme *CgULP1*, SUMO-activating enzymes *CgAOS1* and *CgUBA2,* and SUMO-conjugating enzyme *CgUBC9*, suggesting that these, like in *S. cerevisiae*, could also be essential in *C. glabrata*.

An initial examination of the SUMO proteome in *C. glabrata* revealed several proteins to be SUMOylated. Lack of SUMO ligases, CgSiz1 and CgSiz2, led to loss of the majority of SUMOylation (see Fig. 8*A*), although their increased dosage resulted in accumulation of additional SUMO-conjugated proteins (see Fig. 8*B*). Interestingly, we observed several high molecular weight SUMOylated proteins with additional copies of CgSiz2 (see Fig. 8*B*) suggesting that, as in *S. cerevisiae* (45), CgSiz2 may also be involved in polySUMOylation in *C. glabrata*. SUMOylation pattern studies in the *Cgulp2*Δ mutant revealed intriguing results as, surprisingly, we could neither detect SUMOylated proteins nor the SUMO protein in the mutant (see Fig. 8*A*). We reasoned that there maybe two possible explanations for this observation as follows. First, CgUlp2 is the SUMO-processing enzyme and therefore, in the absence of mature SUMO, no sumoylation takes place. Second, in the *Cgulp2*Δ mutant, SUMOylated proteins accumulate and are targeted for degradation by the SUMO-dependent ubiquitination pathway. Our experiments to test these possibilities suggest that CgUlp2 is unlikely to be the processing enzyme because introduction of the processed SUMO does not completely alleviate *Cgulp2*Δ phenotypes. Similarly, inhibition of proteasome also does not completely rescue the phenotype. However, both treatments improve *Cgulp2*Δ growth perceptibly suggesting that tilting the balance toward retaining SUMOylated proteins can improve *Cgulp2*Δ phenotypes. It further suggests that lack of a SUMOylated protein rather than deSUMOylating a critical protein(s) as a cause for *Cgulp2*Δ mutant phenotypes cannot be ruled out.

Three lines of evidence indicate an important role for SUMOylation in cellular stress response in *C. glabrata*. First, perturbing SUMOylation by deleting SUMO ligases CgSiz1 and CgSiz2 or deSUMOylating enzyme CgUlp2 resulted in diminished survival under different stress conditions (see Fig. 4, *B* and *C*). Second, *C. glabrata* cells respond to a changing environment, including ethanol stress and macrophage internal milieu by SUMOylating multiple cellular proteins (see Fig. 10). Third, the *C. glabrata* mutant disrupted for *CgULP2* exhibited altered cell morphology and cell wall architecture and the constitutively active terminal MAPK (CgSlt2) of the cell wall integrity signaling pathway (see Fig. 5). These findings along with strong survival defects of the *Cgulp2*Δ mutant in specific tissues in the disseminated candidiasis model (see Fig. 11, *C–E*) indicate that SUMOylation is pivotal to stress response in *C. glabrata*.

The fungal cell wall is a dynamic organelle, and any alterations to its core constituents (β-glucan, chitin, and mannoproteins) result in the activation of compensatory mechanism(s) (37). The *Cgulp2*Δ mutant contained elevated levels of chitin in the cell wall (Fig. 5*C*). Importantly, an increase in the cell wall chitin content has previously been associated with reduced susceptibility to the β-1,3-glucan synthesis-targeting echinocandin antifungals and diminished virulence in *C. albicans* (46, 47). However, despite elevated chitin levels, the *Cgulp2*Δ mutant was found to not be resistant to caspofungin (see Fig. 4*C*). Of note, *C. glabrata* mutants with perturbed SUMOylation (*Cgsiz1*Δ, *Cgsiz2*Δ, *Cgsiz1*Δ*Cgsiz2*Δ, and *Cgulp2*Δ) did not exhibit altered sensitivity to the ergosterol biosynthesis inhibitor, fluconazole, either (see Fig. 4*C*). Consistently, cellular SUMOylation status remained unaffected upon exposure of *C. glabrata* cells to fluconazole (see Fig. 10*A*) suggesting that SUMOylation is dispensable for response of *C. glabrata* cells to azole and echinocandin antifungal drugs.

An important feature of this work is the strong conservation of the SUMOylation pathway between *S. cerevisiae* and *C. glabrata*. Similar to *S. cerevisiae* (48, 49), SUMOylation appears to be involved in the regulation of the telomere position effect in *C. glabrata*. Adherence to the host tissue, an important virulence attribute of *C. glabrata*, is mediated by a large family of cell wall proteins, including Epa adhesins (30, 40). The majority of the adhesin-encoding *EPA* genes in *C. glabrata* are transcriptionally silenced due to their close proximity to telomeres (40–42). SUMOylation is a reversible process, and the tight regulation of SUMO conjugation and SUMO removal is probably necessary to fine-tune substrate functions (1, 2). Our finding that a lack of the CgUlp2 deSUMOylase resulted in further repression of *EPA1* and *EPA6* expression and hypoadherence (see Fig. 6, *A* and *B*) indicates that removal of the SUMO modification from component(s) of the subtelomeric silencing machinery is probably pivotal to the expression of subtelomeric genes. This is particularly relevant for the virulence of *C. glabrata* due to the subtelomere-based localization of *EPA* genes that are likely to be relieved of the telomere position effect in response to host environmental cues. Notably, transcriptional activation of *EPA6*, which is required for biofilm formation, has been shown to be regulated by niacin levels in the mouse model of urinary tract infection (47, 50).

Taken together, our findings demonstrate for the first time a pivotal role for SUMOylation in the life cycle of *C. glabrata*.

Experimental Procedures

Strains and Culture Conditions—Bacterial and *C. glabrata* strains were routinely maintained in the LB medium (1% tryptone, 0.5% yeast extract, and 1% NaCl) at 37 °C and YPD (1% yeast extract, 2% peptone, and 2% dextrose) medium at 30 °C, respectively. For alternative carbon source utilization, the synthetically defined YNB (0.67% YNB and 2% dextrose) medium was used. *C. glabrata* cultures were grown in the CAA medium (0.67% yeast nitrogen base (YNB) without amino acids, 0.6% casamino acids, and 2% dextrose) for adherence analysis. Logarithmic (log) phase *C. glabrata* cells were obtained after incubation of overnight cultures for 4 h in the fresh medium at 30 °C with shaking at 200 rpm. *S. cerevisiae* strains were routinely grown either in YPD medium or minimal medium lacking the indicated nutrient. Bacterial, *S. cerevisiae,* and *C. glabrata* strains and plasmids used in this study are listed in Table 2.

TABLE 2
List of strains and plasmids used in the study

Strain	Genotype	Reference
YRK19	*ura3::Tn903 G418^R*	(57)
YRK20	*URA3* or *Cg462*	(58)
YRK949	*URA3 Cgsiz1Δ::nat1*	This study
YRK950	*URA3 Cgsiz2Δ::nat1*	This study
YRK1042	*URA3 Cgsiz1Δ::nat1 Cgsiz2Δ::hph*	This study
YRK971	*URA3 Cgulp2Δ::nat1*	This study
YRK999	*ura3::Tn903 G418^R Cgsiz1Δ::nat1*	This study
YRK1000	*ura3::Tn903 G418^R Cgsiz2Δ::nat1*	This study
YRK1064	*ura3::Tn903 G418^R Cgsiz1Δ::nat1 Cgsiz2Δ::hph*	This study
YRK990	*ura3::Tn903 G418^R Cgulp2Δ::nat1*	This study
YRK1057	*ura3::Tn903 G418^R/pRK74*	This study
YRK1058	*ura3::Tn903 G418^R Cgsiz2Δ::nat1/pRK74*	This study
YRK1059	*ura3::Tn903 G418^R Cgulp2Δ::nat1/pRK74*	This study
YRK1060	*ura3::Tn903 G418^R Cgsiz2Δ::nat1/pCKM381*	This study
YRK1061	*ura3::Tn903 G418^R Cgulp2Δ::nat1/pCKM382*	This study
YRK1074	*ura3::Tn903 G418^R Cgsiz1Δ::nat1/pRK74*	This study
YRK1075	*ura3::Tn903 G418^R Cgsiz1Δ::nat1/pRK1071*	This study
YRK1106	*ura3::Tn903 G418^R Cgsiz2Δ::nat1 Cgsiz2Δ::hph/pRK74*	This study
YRK1108	*ura3::Tn903 G418^R Cgsiz2Δ::nat1 Cgsiz2Δ::hph/pCKM377*	This study
YRK1110	*ura3::Tn903 G418^R Cgsiz2Δ::nat1 Cgsiz2Δ::hph/pCKM381*	This study
YRK1020	*ura3::Tn903 G418^R/pCKM379*	This study
YRK1022	*ura3::Tn903 G418^R Cgsmt3::hph/pCKM379*	This study
KRC6	*smt3::hyg/pCKM405*	This study
KRY1502	*Sculp2::His3 TEL URA*	This study
KRY968	BY 4743; *Scsmt3::*kanMX4/SMT3	Euroscarf
Plasmid	**Description**	**Reference**
pRK74	pGRB2.2, CEN-ARS plasmid with *S. cerevisiae URA3* as selection marker. MCS sites are located between *S. cerevisiae PGK1* promotor and 3' UTR of *HIS3*	(59)
pRK77	pAP599, Plasmid with *S. cerevisiae URA3* and *hph* expression cassette which confers hygromycin resistance. *Hph* gene is flanked with *PGK1* promotor at 5' end and 3' UTR of *HIS3* at other end and entire cassette is flanked by MCS sites.	(60)
pRK625	pCR2.1 plasmid containing the *nat1* gene	Cormack laboratory
pRK983	*CgSMT3* 5' UTR cloned in pAP599	This study
pRK985	*CgSMT3* 5' UTR and 3' UTR cloned in pAP599	This study
pRK986	*CgSIZ2* 5' UTR cloned in pAP599	This study
pRK990	*CgSIZ2* 5' UTR and 3' UTR cloned in pAP599	This study
pRK1001	pCN-PDC1-a high expression promoter with *nat1* gene	Addgene plasmid # 45325
pCKM377	*CgSIZ1* cloned in pRK74	This study
pCKM379	*CgSMT3* cloned in pRK74	This study
pCKM381	*CgSIZ2* cloned in pRK74	This study
pCKM382	*CgULP2* cloned in pRK74	This study
pCKM387	*CgULP1* cloned in pBEVY-T	This study
pCKM394	*CgSMT3* cloned in pBEVY-L	This study
pCKM405	6XHIS3XFLAG tagged *CgSMT3* in pRK1001	This study
pCKM428	6XHIS3XFLAG tagged *CgSIZ2* in pRK74	This study
pCKM430	6XHIS3XFLAG tagged *CgULP1* in pRK74	This study
pCKM431	6XHIS3XFLAG tagged *CgULP2* in pRK74	This study
pCKM432	6XHIS3XFLAG tagged *CgSIZ1* in pRK74	This study
pCKM469	6XHIS3XFLAG modified *CgSMT3* in pRK1001	This study

Construction of C. glabrata Deletion Strains and Plasmids—*C. glabrata siz1*Δ, *siz2*Δ, and *ulp2*Δ strains were created using the homologous recombination-based strategy as described previously (51). For generation of the *Cgsiz1*Δ*siz2*Δ strain, 433 and 406 bp of 5′UTR and 3′UTR regions, respectively, of the *CgSIZ2* ORF were cloned in the pAP599 plasmid in such a way that *CgSIZ2* UTRs flank each end of the *hph1* gene. The 2.96-kb fragment containing 5′UTR-*CgSIZ2*, *hph1* gene, and 3′UTR-*CgSIZ2* was obtained by digestion of the plasmid pRK990 with KpnI and SacI restriction enzymes and transformed into the *Cgsiz1*Δ::*nat1* strain via the lithium acetate method. Transformants were selected on the YPD medium containing hygromycin and confirmed for disruption of the *CgSIZ2* ORF with the *hph1* gene via PCR. To generate the *Cgsmt3*Δ/*CgSMT3* strain, *C. glabrata* wild-type strain (YRK19) was first transformed with the plasmid pRK1069 containing full-length *CgSMT3* gene under the *PGK1* promoter. Transformants were selected for uracil prototrophy and colony purified followed by replacement of the genomic *CgSMT3* locus with the *hph1* gene. Disruption of the genomic *CgSMT3* locus in the YRK1020 strain was achieved by transforming with a linear DNA fragment (3.91 kb), carrying 5′UTR-*CgSMT3*, *hph1* gene, and 3′UTR-*CgSMT3*, obtained from the XhoI and SacI-digested pRK985 plasmid. Hygromycin-resistant colonies were checked for disruption of the *CgSMT3* ORF with the *hph1* gene via PCR.

All plasmids encoding *C. glabrata* genes were constructed by amplifying sequence-encoding full-length protein from genomic DNA and placed downstream of the *PGK1* promoter in pRK74 plasmid. The His_6-3×FLAG tags were constructed by first ligating an oligonucleotide encoding three copies of the FLAG sequence in the NheI/BamHI site of pRSETa plasmid (Invitrogen). Then the cassette containing His-FLAG was isolated as an XbaI/BamHI fragment and placed downstream of the *PGK1* promoter in the pRK74 plasmid. For tagging of *C. glabrata* proteins at the N terminus, *C. glabrata* genes were placed in-frame with the His-FLAG sequence in the pRK74 plasmid. Construct encoding mature SUMO was made by amplifying the coding region of *SMT3* until the diglycine motif and including a stop codon in the reverse primer. Sequence of primers used and further details are available upon request.

Microscopy Analysis—For differential interference contrast (DIC) microscopy, YPD medium-grown overnight cultures of wild-type (WT) and *Cgulp2*Δ strains were inoculated in the fresh YPD medium to an A_{600} of 0.1. After 48–72 h of growth at 30 °C, cells were washed twice with sterile PBS, suspended in PBS, and visualized using the Nikon eclipse 80i microscope (×100 oil immersion objective). For calcofluor white staining, 1 ml of the above-prepared cultures were fixed with 4% formaldehyde for 2 h at room temperature, washed three times, and suspended in PBS. A 4-μl cell suspension was stained with 1 μl of calcofluor white (1 mg/ml solution) and imaged using the confocal microscope (Carl Zeiss LSM 700).

Immunofluorescence was performed with a slight modification to the procedure described earlier (48). Briefly, overnight cultures were subcultured to 0.5–0.6 A_{600} and spun down at 3000 ×*g* for 5 min. After washing with sterile water, cells were suspended in 200 μl of 10 mM DTT and 0.1 M EDTA-KOH and incubated at 30 °C for 10 min. Cells were collected by centrifugation and resuspended in 500 μl of YPD containing 1.2 M sorbitol. 50 μl of 2.5 mg/ml zymolyase and a pinch of lyticase was added to the cell suspension and incubated at 30 °C for 45 min. Spheroplasting was monitored under a light microscope, and when complete, the cells were harvested by spinning at 2000 ×*g* for 10 min and washed three times with YPD medium containing 1.2 M sorbitol. Finally, the spheroplasts were resuspended in 100 μl of YPD supplemented with 1.2 M sorbitol. Immunofluorescence was performed as described earlier (48). Imaging was done in Zeiss Axio Scope A1 microscope equipped with an AxioCam camera and processed using the Zen software.

Quantitative Real Time PCR—*C. glabrata* strains were grown in the YPD medium for 48 h followed by incubation in fresh YPD medium for 1 h. Cells were collected, and RNA was extracted using the acid phenol extraction method. First-strand cDNA synthesis was done using the SuperScript III First-Strand Synthesis System for RT-PCR (Invitrogen), and quantitative PCR was performed using the SYBR Green Master Mix (Eurogentec). *CgGAPDH* (glyceraldehyde-3-phosphate dehydrogenase) mRNA was used to normalize RT-quantitative PCR data.

Western Blot—Whole cell extracts were made from overnight *C. glabrata* cultures using trichloroacetic acid (TCA) precipitation (49). An equal number of cells as measured by absorbance were used for protein extractions, and protein levels in samples were estimated by SDS-PAGE/Ponceau-stained blots and, in some cases, additionally by Pierce BCA kit. Protein samples were separated on 10% SDS-PAGE and transferred onto PVDF membrane. After blocking with 3% skimmed milk powder for 1 h, membrane was incubated with FLAG primary antibody (Sigma, 1:10,000) for 1 h, washed three times with TBST, and incubated with the mouse HRP-conjugated secondary antibody (Jackson ImmunoResearch, 1:15,000) for 1 h. Blots were washed three times with TBST and developed with chemiluminal developing solutions from G-Biosciences.

Chitin Estimation—Overnight cultures were inoculated in the YPD medium to an A_{600} of 0.1 and incubated at 30 °C for 6 h. Cells were washed twice with PBS, normalized to an A_{600} of 2.0, and incubated with 2.5 μl of calcofluor white solution (10 mg/ml) for 15 min at room temperature in the dark. After two PBS washes, 12.5 μl of cell suspension (~50,000 yeast cells) was diluted 24-fold in PBS and used to measure mean fluorescence intensity via flow cytometry (BD FACS ARIA III). Mean fluorescence intensity ratio was calculated by dividing the fluorescence intensity value of the mutant sample with that of the WT sample.

Biofilm Assay—The ability of *C. glabrata* cells to produce biofilms on polystyrene-coated plates was assessed as described previously (52). One ml of the YPD-grown logarithmic culture (1×10^5 cells in PBS) was added to a well of the polystyrene-coated 24-well plate and incubated at 37 °C for 90 min. After two PBS washes, 1 ml of the RPMI 1640 medium containing 10% FBS was added to each well, and the plate was incubated at 37 °C with shaking (75 rpm). After 24 h, 500 μl of the spent medium was replaced with the fresh RPMI 1640 medium, and incubation was continued for another 24 h. Unbound *C. glabrata* cells were removed with three PBS washes, and the plate was air-dried for 45 min and incubated with 250 μl of

crystal violet solution (0.4% in 20% ethanol) for 45 min. Well attached *C. glabrata* cells were washed four times with PBS to eliminate surplus crystal violet stain and incubated with 95% ethanol for 45 min. Absorbance of the 100-μl destaining solution was recorded at 595 nm, which is reflective of the number of biofilm-forming *C. glabrata* cells. Absorbance values of wells without *C. glabrata* cells were subtracted from those of yeast-containing wells, and the biofilm ratio was calculated by dividing the mutant absorbance units by those of WT cells.

THP-1 Macrophage Infection—THP-1 monocytes seeded at a density of 1×10^6 per well of a 24-well tissue culture plate were treated with 16 nM phorbol 12-myristate 13-acetate for 12 h followed by infection with *C. glabrata* strains to a multiplicity of infection of 0.1. After 2 h, the wells were washed three times with PBS to remove extracellular yeast cells. THP-1 cells were lysed in water, and the number of intracellular *C. glabrata* cells was determined by plating appropriate dilutions of lysates on rich medium.

Mouse Infection Assay—Experiments involving mice were performed at the Centre for DNA Fingerprinting and Diagnostics animal facility, VIMTA Labs Ltd., Hyderabad, India (www.vimta.com), in strict accordance with the guidelines of The Committee for the Purpose of Control and Supervision of Experiments on Animals, Government of India. The protocol was approved by the Institutional Animal Ethics Committee of the Vimta Labs Ltd. (Institutional Animal Ethics Committee protocol approval number PCD/CDFD/05). YPD medium-grown *C. glabrata* cells (4×10^7, 100 μl of PBS cell suspension) were injected into 6–8-week-old female BALB/c mice through the tail vein. At day 7 post-infection, mice were sacrificed, and three target organs, kidneys, liver, and spleen, were collected. Organs were homogenized in 1 ml of sterile PBS, and organ fungal load was determined by plating appropriate homogenate dilutions on the YPD medium containing penicillin and streptomycin.

Other Procedures—*S. cerevisiae* proteins were retrieved from the Saccharomyces Genome Database, and their orthologues in *C. glabrata* were searched for using Blastp. Percent similarity and identity were calculated using EMBOSS Stretcher (pairwise sequence alignment) tool (53). The protein sequences were scanned for annotated domains using Pfam and HMMER. Maps of proteins along with their domains were generated using DOG (Domain Graph) (54). Zymolyase digestion, CgSlt2 phosphorylation, and adherence analysis were performed as described previously (38, 51).

Author Contributions—R. G., S. V., K. K., S. S. T., K. M., and R. K. conceived the experiments. R. G., S. V., and K. K. performed the experiments. R. G., S. V., K. M., and R. K. analyzed the data and wrote the manuscript.

Acknowledgments—We are grateful to Sridhar and Jayant Pundalikrao Hole for their help with BALB/c mice experiments. We also thank Hita Garapati for sequence comparisons and V. Joy Prashant and A. Lakshmi Annapurna for help with confocal microscopy.

References

1. Geiss-Friedlander, R., and Melchior, F. (2007) Concepts in sumoylation: a decade on. *Nat. Rev. Mol. Cell Biol.* **8,** 947–956
2. Wilkinson, K. A., and Henley, J. M. (2010) Mechanisms, regulation and consequences of protein SUMOylation. *Biochem. J.* **428,** 133–145
3. Wang, Y., and Dasso, M. (2009) SUMOylation and deSUMOylation at a glance. *J. Cell Sci.* **122,** 4249–4252
4. Flotho, A., and Melchior, F. (2013) Sumoylation: a regulatory protein modification in health and disease. *Annu. Rev. Biochem.* **82,** 357–385
5. Dohmen, R. J., Stappen, R., McGrath, J. P., Forrová, H., Kolarov, J., Goffeau, A., and Varshavsky, A. (1995) An essential yeast gene encoding a homolog of ubiquitin-activating enzyme. *J. Biol. Chem.* **270,** 18099–18109
6. Johnson, E. S., Schwienhorst, I., Dohmen, R. J., and Blobel, G. (1997) The ubiquitin-like protein Smt3p is activated for conjugation to other proteins by an Aos1p/Uba2p heterodimer. *EMBO J.* **16,** 5509–5519
7. Johnson, E. S., and Blobel, G. (1997) Ubc9p is the conjugating enzyme for the ubiquitin-like protein Smt3p. *J. Biol. Chem.* **272,** 26799–26802
8. Li, S. J., and Hochstrasser, M. (1999) A new protease required for cell-cycle progression in yeast. *Nature* **398,** 246–251
9. Ouspenski, I. I., Elledge, S. J., and Brinkley, B. R. (1999) New yeast genes important for chromosome integrity and segregation identified by dosage effects on genome stability. *Nucleic Acids Res.* **27,** 3001–3008
10. Li, S. J., and Hochstrasser, M. (2000) The yeast ULP2 (SMT4) gene encodes a novel protease specific for the ubiquitin-like Smt3 protein. *Mol. Cell. Biol.* **20,** 2367–2377
11. Takahashi, Y., Kahyo, T., Toh-E, A., Yasuda, H., and Kikuchi, Y. (2001) Yeast Ull1/Siz1 is a novel SUMO1/Smt3 ligase for septin components and functions as an adaptor between conjugating enzyme and substrates. *J. Biol. Chem.* **276,** 48973–48977
12. Yeh, E. T. (2009) SUMOylation and De-SUMOylation: wrestling with life's processes. *J. Biol. Chem.* **284,** 8223–8227
13. Li, S. J., and Hochstrasser, M. (2003) The Ulp1 SUMO isopeptidase: distinct domains required for viability, nuclear envelope localization, and substrate specificity. *J. Cell Biol.* **160,** 1069–1081
14. Reindle, A., Belichenko, I., Bylebyl, G. R., Chen, X. L., Gandhi, N., and Johnson, E. S. (2006) Multiple domains in Siz SUMO ligases contribute to substrate selectivity. *J. Cell Sci.* **119,** 4749–4757
15. Bylebyl, G. R., Belichenko, I., and Johnson, E. S. (2003) The SUMO isopeptidase Ulp2 prevents accumulation of SUMO chains in yeast. *J. Biol. Chem.* **278,** 44113–44120
16. Wohlschlegel, J. A., Johnson, E. S., Reed, S. I., and Yates, J. R., 3rd (2004) Global analysis of protein sumoylation in *Saccharomyces cerevisiae*. *J. Biol. Chem.* **279,** 45662–45668
17. Wykoff, D. D., and O'Shea, E. K. (2005) Identification of sumoylated proteins by systematic immunoprecipitation of the budding yeast proteome. *Mol. Cell. Proteomics* **4,** 73–83
18. Hannich, J. T., Lewis, A., Kroetz, M. B., Li, S. J., Heide, H., Emili, A., and Hochstrasser, M. (2005) Defining the SUMO-modified proteome by multiple approaches in *Saccharomyces cerevisiae*. *J. Biol. Chem.* **280,** 4102–4110
19. Denison, C., Rudner, A. D., Gerber, S. A., Bakalarski, C. E., Moazed, D., and Gygi, S. P. (2005) A proteomic strategy for gaining insights into protein sumoylation in yeast. *Mol. Cell. Proteomics* **4,** 246–254
20. Zhou, W., Ryan, J. J., and Zhou, H. (2004) Global analyses of sumoylated proteins in *Saccharomyces cerevisiae*. Induction of protein sumoylation by cellular stresses. *J. Biol. Chem.* **279,** 32262–32268
21. Abu Irqeba, A., Li, Y., Panahi, M., Zhu, M., and Wang, Y. (2014) Regulating global sumoylation by a MAP kinase Hog1 and its potential role in osmotolerance in yeast. *PLoS One* **9,** e87306
22. Leach, M. D., Stead, D. A., Argo, E., and Brown, A. J. (2011) Identification of sumoylation targets, combined with inactivation of SMT3, reveals the impact of sumoylation upon growth, morphology, and stress resistance in the pathogen *Candida albicans*. *Mol. Biol. Cell* **22,** 687–702
23. Pfaller, M. A., and Diekema, D. J. (2007) Epidemiology of invasive candidiasis: a persistent public health problem. *Clin. Microbiol. Rev.* **20,** 133–163
24. Pappas, P. G., Alexander, B. D., Andes, D. R., Hadley, S., Kauffman, C. A.,

Freifeld, A., Anaissie, E. J., Brumble, L. M., Herwaldt, L., Ito, J., Kontoyiannis, D. P., Lyon, G. M., Marr, K. A., Morrison, V. A., Park, B. J., *et al.* (2010) Invasive fungal infections among organ transplant recipients: results of the Transplant-Associated Infection Surveillance Network (TRANSNET). *Clin. Infect. Dis.* **50,** 1101–1111

25. Pfaller, M., Neofytos, D., Diekema, D., Azie, N., Meier-Kriesche, H. U., Quan, S. P., and Horn, D. (2012) Epidemiology and outcomes of candidemia in 3648 patients: data from the Prospective Antifungal Therapy (PATH Alliance(R)) registry, 2004–2008. *Diagn. Microbiol. Infect. Dis.* **74,** 323–331
26. Pfaller, M. A., Moet, G. J., Messer, S. A., Jones, R. N., and Castanheira, M. (2011) Candida bloodstream infections: comparison of species distributions and antifungal resistance patterns in community-onset and nosocomial isolates in the SENTRY Antimicrobial Surveillance Program, 2008–2009. *Antimicrob. Agents Chemother.* **55,** 561–566
27. Montagna, M. T., Lovero, G., Borghi, E., Amato, G., Andreoni, S., Campion, L., Lo Cascio, G., Lombardi, G., Luzzaro, F., Manso, E., Mussap, M., Pecile, P., Perin, S., Tangorra, E., Tronci, M., Iatta, R., and Morace, G. (2014) Candidemia in intensive care unit: a nationwide prospective observational survey (GISIA-3 study) and review of the European literature from 2000 through 2013. *Eur. Rev. Med. Pharmacol. Sci.* **18,** 661–674
28. Klevay, M. J., Ernst, E. J., Hollanbaugh, J. L., Miller, J. G., Pfaller, M. A., and Diekema, D. J. (2008) Therapy and outcome of *Candida glabrata versus Candida albicans* bloodstream infection. *Diagn. Microbiol. Infect. dis.* **60,** 273–277
29. Moran, C., Grussemeyer, C. A., Spalding, J. R., Benjamin, D. K., Jr., and Reed, S. D. (2010) Comparison of costs, length of stay, and mortality associated with *Candida glabrata* and *Candida albicans* bloodstream infections. *Am. J. Infect. Control* **38,** 78–80
30. Rodrigues, C. F., Silva, S., and Henriques, M. (2014) *Candida glabrata*: a review of its features and resistance. *Eur. J. Clin. Microbiol. Infect. Dis.* **33,** 673–688
31. Harting, R., Bayram, O., Laubinger, K., Valerius, O., and Braus, G. H. (2013) Interplay of the fungal sumoylation network for control of multicellular development. *Mol. Microbiol.* **90,** 1125–1145
32. Takahashi, Y., and Kikuchi, Y. (2005) Yeast PIAS-type Ull1/Siz1 is composed of SUMO ligase and regulatory domains. *J. Biol. Chem.* **280,** 35822–35828
33. Johnson, E. S., and Gupta, A. A. (2001) An E3-like factor that promotes SUMO conjugation to the yeast septins. *Cell* **106,** 735–744
34. Takahashi, Y., Iwase, M., Strunnikov, A. V., and Kikuchi, Y. (2008) Cytoplasmic sumoylation by PIAS-type Siz1-SUMO ligase. *Cell Cycle* **7,** 1738–1744
35. Darst, R. P., Garcia, S. N., Koch, M. R., and Pillus, L. (2008) Slx5 promotes transcriptional silencing and is required for robust growth in the absence of Sir2. *Mol. Cell. Biol.* **28,** 1361–1372
36. Zhao, X., and Blobel, G. (2005) A SUMO ligase is part of a nuclear multiprotein complex that affects DNA repair and chromosomal organization. *Proc. Natl. Acad. Sci. U.S.A.* **102,** 4777–4782
37. Bowman, S. M., and Free, S. J. (2006) The structure and synthesis of the fungal cell wall. *BioEssays* **28,** 799–808
38. Borah, S., Shivarathri, R., and Kaur, R. (2011) The Rho1 GTPase-activating protein CgBem2 is required for survival of azole stress in *Candida glabrata*. *J. Biol. Chem.* **286,** 34311–34324
39. Cormack, B. P., Ghori, N., and Falkow, S. (1999) An adhesin of the yeast pathogen *Candida glabrata* mediating adherence to human epithelial cells. *Science* **285,** 578–582
40. de Groot, P. W., Bader, O., de Boer, A. D., Weig, M., and Chauhan, N. (2013) Adhesins in human fungal pathogens: glue with plenty of stick. *Eukaryot. Cell* **12,** 470–481
41. Castaño, I., Pan, S. J., Zupancic, M., Hennequin, C., Dujon, B., and Cormack, B. P. (2005) Telomere length control and transcriptional regulation of subtelomeric adhesins in *Candida glabrata*. *Mol. Microbiol.* **55,** 1246–1258
42. Iraqui, I., Garcia-Sanchez, S., Aubert, S., Dromer, F., Ghigo, J. M., d'Enfert, C., and Janbon, G. (2005) The Yak1p kinase controls expression of adhesins and biofilm formation in *Candida glabrata* in a Sir4p-dependent pathway. *Mol. Microbiol.* **55,** 1259–1271
43. Sydorskyy, Y., Srikumar, T., Jeram, S. M., Wheaton, S., Vizeacoumar, F. J., Makhnevych, T., Chong, Y. T., Gingras, A. C., and Raught, B. (2010) A novel mechanism for SUMO system control: regulated Ulp1 nucleolar sequestration. *Mol. Cell. Biol.* **30,** 4452–4462
44. Tanaka, K., Nishide, J., Okazaki, K., Kato, H., Niwa, O., Nakagawa, T., Matsuda, H., Kawamukai, M., and Murakami, Y. (1999) Characterization of a fission yeast SUMO-1 homologue, pmt3p, required for multiple nuclear events, including the control of telomere length and chromosome segregation. *Mol. Cell. Biol.* **19,** 8660–8672
45. D'Ambrosio, L. M., and Lavoie, B. D. (2014) Pds5 prevents the PolySUMO-dependent separation of sister chromatids. *Curr. Biol.* **24,** 361–371
46. Walker, L. A., Munro, C. A., de Bruijn, I., Lenardon, M. D., McKinnon, A., and Gow, N. A. (2008) Stimulation of chitin synthesis rescues *Candida albicans* from echinocandins. *PLoS Pathog.* **4,** e1000040
47. Ben-Ami, R., Garcia-Effron, G., Lewis, R. E., Gamarra, S., Leventakos, K., Perlin, D. S., and Kontoyiannis, D. P. (2011) Fitness and virulence costs of *Candida albicans* FKS1 hot spot mutations associated with echinocandin resistance. *J. Infect. Dis.* **204,** 626–635
48. Pasupala, N., Easwaran, S., Hannan, A., Shore, D., and Mishra, K. (2012) The SUMO E3 ligase Siz2 exerts a locus-dependent effect on gene silencing in *Saccharomyces cerevisiae*. *Eukaryot. Cell* **11,** 452–462
49. Hannan, A., Abraham, N. M., Goyal, S., Jamir, I., Priyakumar, U. D., and Mishra, K. (2015) Sumoylation of Sir2 differentially regulates transcriptional silencing in yeast. *Nucleic Acids Res.* **43,** 10213–10226
50. Domergue, R., Castaño, I., De Las Peñas, A., Zupancic, M., Lockatell, V., Hebel, J. R., Johnson, D., and Cormack, B. P. (2005) Nicotinic acid limitation regulates silencing of *Candida adhesins* during UTI. *Science* **308,** 866–870
51. Borah, S., Shivarathri, R., Srivastava, V. K., Ferrari, S., Sanglard, D., and Kaur, R. (2014) Pivotal role for a tail subunit of the RNA polymerase II mediator complex CgMed2 in azole tolerance and adherence in *Candida glabrata*. *Antimicrob. Agents Chemother.* **58,** 5976–5986
52. Djordjevic, D., Wiedmann, M., and McLandsborough, L. A. (2002) Microtiter plate assay for assessment of *Listeria monocytogenes* biofilm formation. *Appl. Environ. Microbiol.* **68,** 2950–2958
53. Rice, P., Longden, I., and Bleasby, A. (2000) EMBOSS: the European molecular biology open software suite. *Trends Genet.* **16,** 276–277
54. Ren, J., Wen, L., Gao, X., Jin, C., Xue, Y., and Yao, X. (2009) DOG 1.0: illustrator of protein domain structures. *Cell Res.* **19,** 271–273
55. Cormack, B. P., and Falkow, S. (1999) Efficient homologous and illegitimate recombination in the opportunistic yeast pathogen *Candida glabrata*. *Genetics* **151,** 979–987
56. De Las Peñas, A., Pan, S. J., Castaño, I., Alder, J., Cregg, R., and Cormack, B. P. (2003) Virulence-related surface glycoproteins in the yeast pathogen Candida glabrata are encoded in subtelomeric clusters and subject to RAP1- and SIR-dependent transcriptional silencing. *Genes Dev.* **17,** 2245–2258
57. Frieman, M. B., McCaffery, J. M., and Cormack, B. P. (2002) Modular domain structure in the *Candida glabrata* adhesin Epa1p, a β1,6 glucan-cross-linked cell wall protein. *Mol. Microbiol.* **46,** 479–492
58. Kaur, R., Ma, B., and Cormack, B. P. (2007) A family of glycosylphosphatidylinositol-linked aspartyl proteases is required for virulence of *Candida glabrata*. *Proc. Natl. Acad. Sci. U.S.A.* **104,** 7628–7633